NOVEL I*N VITRO* METHODS TO UNDERSTAND THE MECHANICAL BEHAVIOR & BIOLOGICAL IMPLICATIONS OF FLUID SHEAR FROM CED DEVICES IN THE BRAIN

By

SWETHA KODAMASIMHAM

A thesis submitted to the

School of Graduate Studies

Rutgers, The State University of New Jersey

In partial fulfillment of the requirements

For the degree of

Master of Science

Graduate Program in Biomedical Engineering

Written under the direction of

Jay C. Sy Ph.D.

And approved by

New Brunswick, New Jersey

October 2018

ABSTRACT OF THE THESIS

Novel *in Vitro* Methods to Understand the Mechanical Behavior & Biological Implications of Fluid Shear from CED Devices in the Brain

By: SWETHA KODAMASIMHAM

Thesis Director: Jay C. Sy, Ph.D.

Convection enhanced delivery (CED) devices are a promising therapeutic strategy to overcome some of the obstacles involved in delivering drugs to the brain. CED devices bypass the blood-brain barrier (BBB), targeting drugs locally into the interstitial spaces using pressure-mediated flow, which can increase drug penetration and efficacy compared to systemic delivery. A critical step in developing brain implants is to investigate how the mechanisms of the device effect the surrounding environment. This can provide insight into any mechanical or biological limitations of the device that need to be considered for implementation into a clinical setting. Although mechanical characterization and inflammation studies have been conducted for other kinds of brain implants, limited work has focused on applying these type of studies to the operation of CED devices specifically. As a result, how pressure-driven flow from CED devices affects local brain tissue is not yet clearly understood. This study implements unique computational and biological techniques to characterize *in vitro* the effects of fluid shear on local deformation and inflammation of brain tissue through both quantitative and spatial analysis. Particle image velocimetry (PIV) is an optical method designed for flow visualization that we translate to the study of fluid shear from CED devices using agarose brain phantoms as a mechanical model of brain tissue. PIV analysis was successfully able to quantify magnitudes of

deformation as a function of distance and time and generate heat maps highlighting areas of most impact from fluid shear in detail that has not been done in the past. This characterization allows for predictions of how mechanical behavior from CED devices can potentially impact biological response. Infusion experiments were also conducted in 3D C8-B4 microglial cultures embedded in Matrigel that can serve as a simple model of the brain parenchyma and evaluated for elevations in tumor necrosis factor alpha (TNF-α) as the candidate inflammatory marker. However, given the small volume of affected cells relative to total cell-gel construct, this bulk quantification method proved ineffective in detecting any overall increased levels of TNF-α compared to positive (lipopolysaccharide (LPS)-treated) and negative (untreated) controls, suggesting that a spatial visualization of inflammation may be a more suitable approach for more local resolution of any biological effects from fluid shear. Using a secretory inhibitor, Brefeldin A (BFA), we develop and optimize a method to retain TNF-α within the cells for cytochemical staining to conduct spatial analysis of cell activation. With this, we accomplish the first step in developing an immunofluorescence technique can be used with the cell model to gain an understanding of spatial resolution of inflammation from fluid shear to eventually correlate with the tissue mechanics studies. Ultimately, these techniques can provide new and better tools for CED device characterization prior to *in vivo* studies.

ACKNOWLEDGMENTS

I would like to thank first and for most my advisor Dr. Jay Sy for all the support and guidance in helping me finish this project and for all the valuable skills that I have developed along the way that I will carry with me in my future endeavors. I would like to thank my committee members Dr. Li Cai and Dr. Kristen Labazzo for their constructive feedback during the review of this thesis. I would like to thank Gemi Dessi who has guided me tremendously throughout the course of this project and has personally been a great source of encouragement for me. I would like to thank everyone in the Sy lab who was made my time here at Rutgers very memorable and made every day fun, worthwhile, and educational; I have learned a lot from each and every one of you. As a tribute to my undergraduate experience here at Rutgers, I would like to also thank The Center of Biomaterials (NJCBM) and Dr. Joachim Kohn, my undergraduate lab and director. This was the place where I first developed an interest in doing research and where I learned many fundamental skills that really kick-started my career. Thank you to my advisors at NJCBM Dr. Sanjeeva Murthy and Dr. Divya Bhatnagar for all their guidance early on in my undergraduate career that motivated me to pursue a Masters in the first place. Lastly, I would like to thank my parents and brother for their support throughout every decision I have made in my life-this would not have been possible without them.

TABLE OF CONTENTS

LIST OF FIGURES

LIST OF TABLES

CHAPTER 1: INTRODUCTION

Implantable convection-enhanced delivery (CED) devices are clinically used in brain drug delivery for treatment of aggressive brain disorders because they can bypass the blood-brain barrier (BBB), allowing for more efficient and targeted delivery. While currently used for cancer treatment primarily, they may also be a promising therapeutic strategy for neurodegenerative and neuropsychiatric disorders as well. There are many studies that have investigated various mechanical stimuli from brain implants and their effects on the surrounding environment, however little is known on how fluid shear from CED devices, in particular, can impact local brain tissue. Two key questions that remain unclear are how brain tissue responds mechanically to different infusion parameters and if the flow alone from these types of devices can cause mechanotransduction of immune cells in the brain. Thus the goals of this thesis are to develop microenvironments that can simulate the mechanical and biological aspects of the the native brain parenchyma *in vitro,* establish methods to determine the effects of wide range fluid shear on tissue mechanics, and explore the implications, if any, of this mechanical behavior on local immune response and cell activation. This information can ultimately provide insight into potential mechanical and biological constraints that need to be considered for both designing and implementation of CED devices for clinical use.

1.1 Targeted Brain Drug Delivery

Recent work has shifted to localized delivery of chemotherapeutics for treatment of aggressive brain disorders such as Glioblastoma Multiforme (GBM) because systemic approaches such as oral delivery have been shown to be inefficient. With a systemic method, it is difficult for drugs to penetrate across the blood-brain barrier (BBB) so only a

small percent of drug actually reaches the target site. This is because the blood-brain barrier is a well protected physical barrier that lacks fenestrations and consists of highly regulated tight junctions and selective transporter molecules as the only means of entry, making it difficult for therapeutic drugs to cross the BBB into the brain parenchyma (**Figure 1.1**) [1]. However, with a more compartmentalized drug delivery approach, the region of interest can be exposed to most of the dose while also decreasing any unwanted effects to other parts of the body. Implantable devices are becoming a promising approach to localized brain drug delivery because they can deliver drugs directly into the interstitial space, bypassing the blood-brain barrier [2].

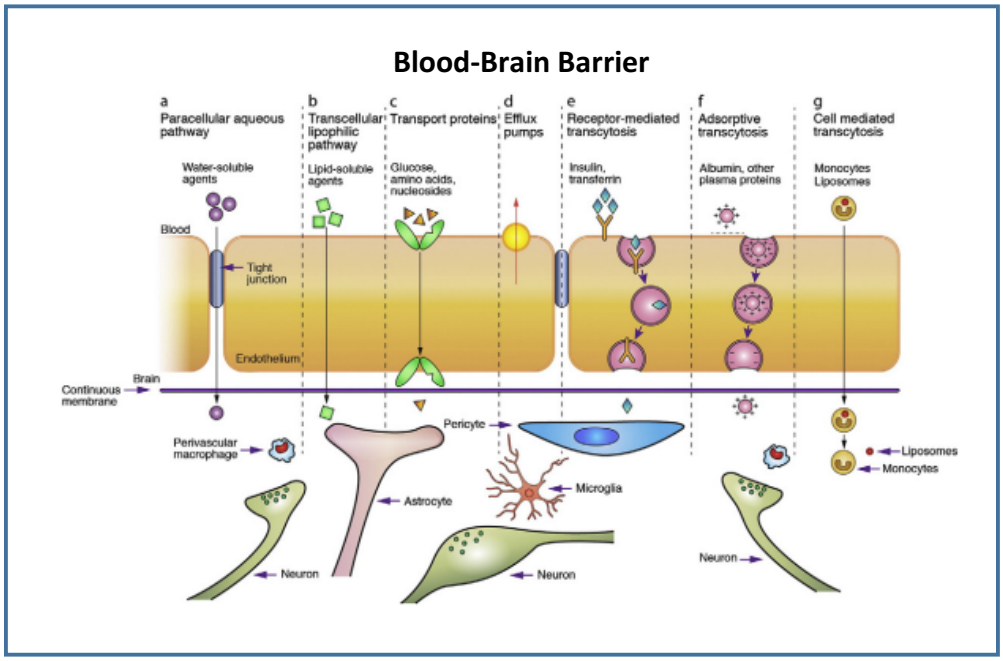

Figure 1.1: *Illustration of the blood-brain barrier and the highly regulated mechanisms that facilitate transport in and out of the brain. Transporting therapeutic agents across the blood brain barrier is arguably one of the greatest obstacles in brain drug delivery [1].*

The Gliadel Wafer is currently the only FDA-approved Central Nervous System (CNS) local delivery device for treatment of GBM. It consists of a polymer matrix that

releases the chemotherapeutic agent carmustine as the polymer matrix degrades. Although moderate success is seen with this approach, studies have shown that high exposure of the drug is achieved only 1-2mm from the implant, making insufficient for long term patient survival [2]. Therefore, there is a need to engineer new implantable devices in order to increase drug penetration.

1.2 Convection Enhanced Delivery

Convection enhanced delivery (CED) devices potentially offer a superior method to directly bypass the the blood-brain barrier. CED uses a positive-pressure infusion of a solute that contains the active drug. The bulk flow is created by a small pressure gradient by a pump that pushes solute through a catheter targeted within the CNS. There are several potential advantages with CED: 1) It can bypass the BBB and can be used to infuse agents with small or large molecular weights via bulk interstitial flow. 2) It provides targeted delivery into the regions where the catheter is placed. 3) It allows for real-time monitoring and adjustments of flow rates. 4) Using CED, it is possible to achieve high infusion rates 5) Unlike diffusion-limited delivery, it provides pressure-driven delivery that enhances interstitial distribution. 6) CED also limits the potential for neurotoxicity because the infusion does not need to be as high as those needed for diffusion-mediated delivery [3].

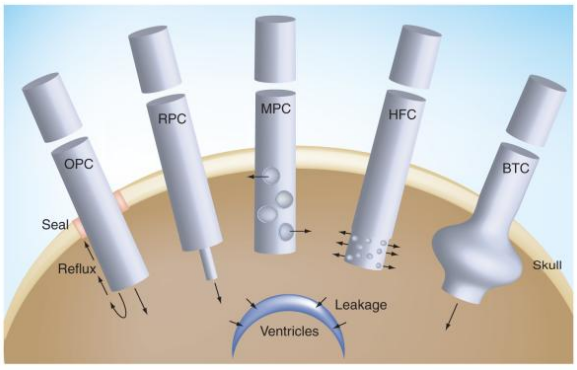

***Figure 2.2**: Schematic of various catheter designs for CED[4] .*

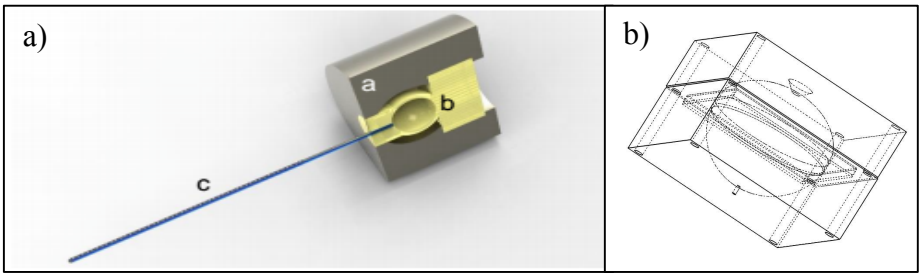

Figure 1.3: *(a) Schematic of the "Micrommaya Reservoir", a CED device currently in development in the Sy Lab for use in a rodent model (b) Computer-aided design (CAD) rendering of the prototype using SolidWorks.*

1.3 *In Vitro* Mechanical Models for Device Characterization

A critical step in developing CED devices and brain implants in general is to understand potential limitations that may impact device design or biocompatibility for eventual clinical use. Brain implants can introduce mechanical forces that may lead to inflammation of surrounding tissue. For example, in literature it is shown that neural probes can cause micromotion within brain tissue or induce cell stretching and these effects have been characterized in many studies [5]. While CED devices are currently only used for applications in oncology, they have potential uses for neurodegenerative and neuropsychiatric disorders as well and therefore it is important to understand how the mechanisms of the device can impact their operation. For CED devices, fluid shear is the main driving force that can play a critical role in altering tissue mechanics and causing an immune response. It has been shown that tissue damage from infusion pressure or strain at the catheter tip can occur if the infusion rate is too high and the tolerable stresses near the injection site are exceeded. Large tissue strains can also cause edema to form near the catheter tip, also leading to poor penetration depths [6,7].

Furthermore, a variety of mechanical cues have been shown to affect cell phenotype. For example, many studies suggest that hemodynamic stress and blood vessel

stiffening can synergistically contribute to changes in cell morphology and behavior by promoting or augmenting atheroprotective signals in aortic endothelial cells, thereby accelerating or slowing down atherosclerosis progression [8]. A similar response has been seen with neural cells when subjected to different surface stiffnesses, suggesting that modifying the surface stiffness of neural implants may minimize adverse reactions and improve biocompatibility [9]. These findings provide support that shifts in mechanical behavior from fluid flow can impact the behavior of cells surrounding the injection site. Fluid shear from infusion has been known to govern drug delivery for CED devices but the biological implications are unclear [10]. Therefore, an in depth characterization of tissue mechanics as a function of fluid shear can be used to compare with inflammation studies aid in establishing infusion parameters that prevent these issues from occurring or at least minimizing their effects for use in a clinical setting.

Additionally, tissue damage can result from backflow along the catheter-tissue interface, a separate issue altogether. Backflow is defined as fluid flow back along the outer surface of a needle or catheter [6] This is a significant problem because the drug will not go to the targeted area or can decrease the drug efficacy. There are several reasons why backflow can occur. In some cases, the catheter can disrupt the tissue, forming space around the outer wall, causing the infusing agent to fill in the void that has been created. This prevents very little pressure flow into the targeted tissue. In addition, intrinsic backflow can be caused by the pressure caused by the infusion. This results in shear forces that disrupt the tissue balance. In order to prevent this, low volumetric flow rates are used [11]. However, there has been no study to the author's knowledge that has directly

correlated the effects of backflow to tissue mechanics and inflammation response to understand these constraints more specifically.

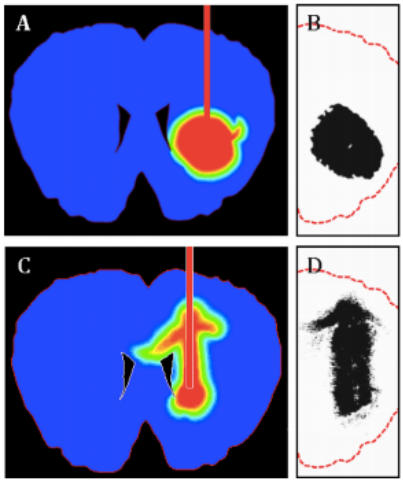

Figure 1.4: *(a) Drug distribution in an ideal case without backflow (b) Drug distribution with the presence of backflow [12].*

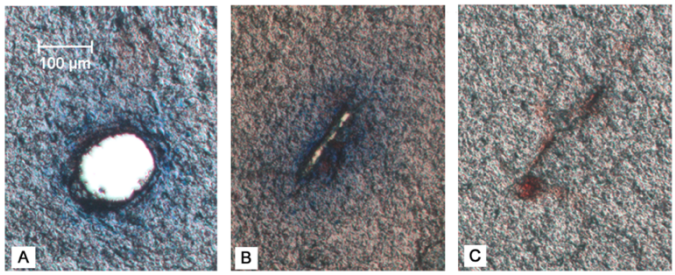

Figure 1.5: *Different types of tissue damage resulting from various CED parameters [6].*

1.3.1 Literature Review of Mechanical Models for Brain Implants

For soft tissues such as the brain, mechanical behavior has been studied using either elastic, viscoelastic, or poroelastic models. Generally, impact models use viscoelasticity whereas long term processes have been modeled using poroelasticity [13]. For CED devices in particular, many studies have used low concentration agarose gels as brain phantoms for studies related to infusion parameters and backflow. These studies have found a direct correlation between infusion parameters such as needle insertion speed and flow rate to backflow [12, 14].

Computational models have also been developed in order to gain a better understanding of tissue mechanics from brain implants. In a study by Levenston, et al. tissue mechanics is characterized using an elastic model to calculate initial strains about an implanted electrode and have shown the relationship between the distance from the implant and the magnitude of deformation [15]. Additionally, a study by Lonser, et al. investigates

the affect of hydrostatic pressure imposed on the tissue by the infusate and correlates strain to catheter diameter and hydrostatic pressure [16]. Furthermore, a 3D finite-element model of the brain was developed to understand the mechanical properties of the probe–tissue interface. Radial and tangential tethering forces were applied and resulted in elevated strain at the tip and shearing along the probe–tissue interface [17].

In more recent times, Cima, et al. have used in vitro gel models to characterize the mechanical behavior of micromotion from neural probes using a new technique called particle image velocimetry to correlate the spatial displacement of fluorescent particles in response to the micromotion and have shown that local strain fields can induce an activation of astrocytes in the brain [18]. The results from this study suggest that this computational technique in particular is promising in that it allows for quick and detailed analysis of tissue deformation. For this reason, we use the methods described in this study as the basis of the technique we develop in our study.

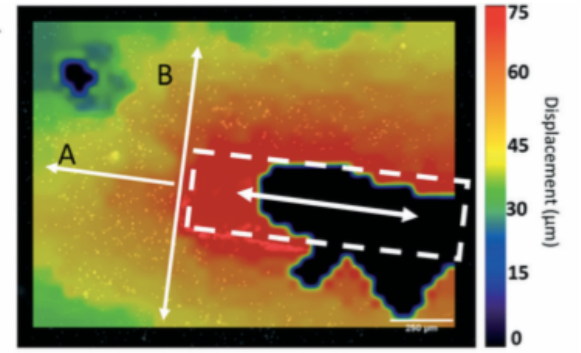

Figure 1.6: *Deformation fields generated from micromotion around a neural probe an in vitro gel model using particle image velocimetry [18].*

1.4 *In Vitro* Cellular Microenvironments for Device Characterization

In addition to understanding any mechanical behavior from brain implants, it also important to understand potential biological limitations that these implants may impose on device design or biocompatibility for eventual clinical use. Often, *in vivo* studies are used

for this purpose and involve performing a craniotomy to insert the device and later sectioning the brain tissue and conducting various immuno-histological analysis to evaluate inflammation response. However, both prototyping the device and conducting these *in vivo* studies can be time consuming and costly. Additionally, *in vivo* models are often complex, making it difficult to understand the cellular response and inflammation pathway. Results from animal studies can also be highly variable because they often depend on factors such as tissue heterogeneity, device placement, and surgical technique [18]. Therefore, developing cellular model where one can simulate some of these effects *in vitro* is beneficial because it can allow for a quick, cost-effective method of screening inflammation due various device parameters in parallel with device development. A simple cell model can elucidate cellular responses on a molecular level and can also be used to evaluate single cell types or fixed ratios of different cell types. As a result, we can gain critical information on the role each cell type plays in contributing to immune response.

1.4.1: 3D Glial Cell Cultures

Many cellular microenvironments have been developed that have allowed simplified modeling of the native brain environment for various types of cell activation studies. The brain consists primarily of neurons and glial cells. Although neurons are responsible for many of the cognitive functions in central nervous system, glial cells accommodate for nearly 90% of the total brain cell population. Microglia and astrocytes, in particular, are two types of glial cells that play a prominent role in inflammation response in the brain. They can get activated as a response to different stimuli both locally and distant and can release various cytokines and chemokines signals [19]. For these reasons, astrocytes and microglia have been the basis for many cell cultures used for cell activation

studies for the brain. For example, a study by Reichert, et al. uses a 2D culture that have examined the glial response to mechanical injury created by a scrape wound [20]. Although planar systems such as this one can resolve many of the cellular responses to stimuli, it has been shown that 3D environments can be more physiologically representative of the brain parenchyma. The 3D structure enables different cell-cell and cell-matrix signaling, allowing it to be potentially be more responsive to secondary injury and trauma. It has also been shown that glial cells in 3D cultures are more quiescent compared to 2D systems and show less signs of cellular stress, allowing for screening in a more dynamic range because the cells are less reactive during the beginning of the experiment [21]. 3D cultures can be developed using different types of basement membrane materials. These membranes help mimic the extracellular matrix of the brain and may contain growth factors that help sustain the cells. Collagen, hyaluronic acid, and Matrigel, to name a few, are some common matrix biomaterials used for the formation of 3D cell cultures. These hydrogels help recreate the spatial arrangement of cells and matrices found in tissue and form a mechanical stiffness that is comparable to the physical environment of the central nervous system [22]. Together, the glial cells and basement membranes form a simple model that can be used for cell activation studies.

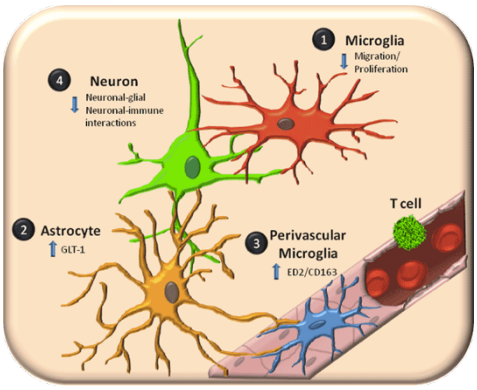

Figure 1.7: *Illustration of the native brain environment comprised of interactions between neurons, microglia, and astrocytes [23]*

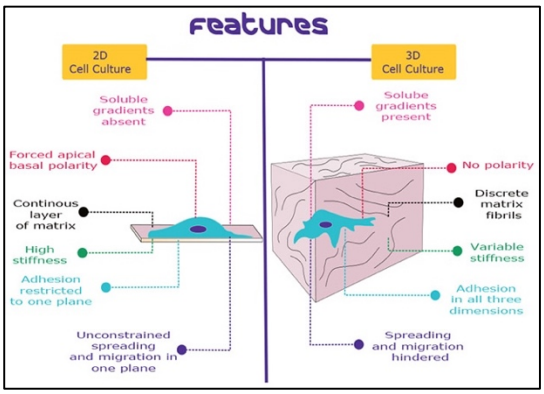

Figure 1.8: *Schematic outlining the differences in characteristics between 2D and 3D cell cultures. This highlights the factors that make 3D cell cultures more physiologically representative of native tissue [24].*

1.4.2: Literature Review of Mechanical Stimulation Studies Using Glial Cultures

There have been many studies that have investigated mechanical stimulation of glial cultures to understand inflammation response and biocompatibility of various types of brain implants. Recent work has focused on stimuli such as micromotion, cyclic straining, and cell stretching as they have many applications in understanding potential adverse tissue responses to neural probes and microelectrodes used for neural prosthetics. Bellamkonda, et al. have explored the cellular responses to electrode induced low-magnitude strain and micromotion. They have developed a cell stretching device to apply low magnitude strain on microglial and astrocyte cultures and have found that applying strains between 1%-5%, have up-regulated biomarkers involved with glial inflammation in stretched astrocytes and microglia. This provides support that low magnitude strains can cause inflammation to brain tissue [5]. Cima, et al. have used 3D collagen cultures to explore the impact of micromotion on astrocyte activation. They have found an increase in glial scarring markers as a response to local micromotion [18]. These results again emphasize the potential effect of a low-end mechanical stimulus on inflammation. It is important to note that while these studies have primarily focused on micromotion, cyclic strain, and stretching, there has been limited work, to the author's knowledge, that has focused on the effect of fluid flow on inflammation of glial cells. While matrix deformation from micromotion can be characterized as rather gradual and cyclic, we can expect to see a more impulsive and bi-directional response from fluid shear as the matrix initially expands radially from the infusion site when fluid shear is introduced and then relaxes after the infusion has ended. As a result, it is clear that this may contribute to differences in mechanical behavior between micromotion and fluid shear. However, despite these

differences, these studies provide support that we can conduct a similar type of study and perhaps see similar results.

1.5 SCIENTIFIC RATIONALE FOR THIS WORK

It has been established thus far that understanding the mechanical behavior and inflammation of brain tissue may play a key role in designing CED devices. In literature, we have seen mechanical models for other brain implants and their implications on tissue damage and inflammation. Brain implants that can cause mechanical stimulation have shown local deformation of brain tissue and increased signs of inflammation markers in *in vivo* and cell studies. *In vitro* cellular microenvironments have been developed to investigate these effects because they can elucidate cellular responses at a molecular level and allow for a fast screening mechanism. However, there is a gap in knowledge of whether fluid shear from CED devices can cause a similar response and induce mechanotransduction of glial cells. Therefore, the purpose of this study is to develop in *vitro* models to determine the effect of fluid shear on the mechanical properties of brain tissue such as tissue deformation. Additionally, a 3D glial model that mimics the brain's immune system *in vitro* will be used to understand how and if these mechanical properties are correlated with inflammation response. Identifying these effects are necessary to determine the feasibility and tolerance of specific infusion rates to use with CED devices to ultimately increase drug penetration for critical brain disorders.

CHAPTER 2: PARTICLE IMAGE VELOCIMTRY FOR QUANTITATIVE AND SPATIAL ANALYSIS OF BRAIN TISSUE MECHANICS FROM FLUID SHEAR

2.1 Motivation

As discussed in Section 1.3, brain implants often induce low magnitude strain that can lead to tissue damage and/or immune activation and there are many studies that have investigated this phenomenon. These studies provide support that fluid shear from CED devices can also have a similar effect but there is limited work that has focused specifically on analyzing the impact of flow on brain tissue. The aim of this section is to understand how fluid shear from CED devices can effect tissue mechanics and drug distribution using an *in vitro*, cell-free model that mimics the mechanical properties of brain tissue and a computational technique called particle image velocimetry (PIV). For a wide range of infusion rates, we quantify the magnitudes of matrix deformation, identify regions of high impact, model the behavior of deformation over time, and compare these results to previous CED backflow studies. Together, this characterization will provide better insight into potential mechanical constraints for various infusion parameters to use with CED devices.

2.2 Experimental Design & Rationale

2.2.1 Development of an Agarose Brain Phantom

Low concentration agarose gel models are widely considered to be a viable *in vitro* model of the physical characteristics of the human brain as mentioned in Section 1.3. These gels have similar poroelasticity to the brain; this makes them useful for evaluating various

infusion parameters that are dependent on poroelasticity such as pressure, volume of distribution, and backflow. Additionally, because these gels are translucent, they can be used to visualize high molecular weight dyes making them useful for infusion studies. Many studies have compared agarose gel models to *in vivo* models and have seen remarkably similar responses, validating their reliability as an accurate *in vitro* model [14]. The brain is an anisotropic tissue can that vary in stiffness [25]. Studies have shown that agarose concentrations between 0.2%-0.6% can reach these different values and achieve similar infusion pressure profiles and drag force by catheter infusion compared to *in vivo* models [14]. Together, these characteristics make agarose gels useful models to mimic the mechanical behavior of brain tissue as a response to fluid shear. For this study, 0.2% agarose brain phantoms are used. We select this concentration because it maximizes the potential of seeing matrix deformation since the stiffness of these phantoms are lower while still being within a range that simulates the mechanical properties of the brain. This also allows for characterization of low stiffness brain tissue, which is the worst possible scenario in a clinical setting.

2.2.2 Quantitative and Spatial Analysis of Matrix Deformation

Agarose brain phantoms were made and embedded with fluorescent beads into a modified well plate that facilitates infusion. A programmable syringe pump is used to infuse 10 μL of water with the following flow rates: 1 μL/min (10 minutes), 10 μL/min (1 minute), 100 μL/min (6 seconds), and 500 μL/min (1.2 seconds). These flow rates were selected because conventionally used parameters found in CED literature range from 0.1 μL/min- 50 μL/min with volumes between 1- 25 μL [12, 26, 27]. This study includes these ranges but also explores flow rates and volumes beyond this range to evaluate the effects

of high infusion rates as well. Time series images were taken before, during, and after infusion and analyzed using particle image velocimetry. Particle image velocimetry (PIV) is an optical method that allows for flow visualization using the signal from the fluorescent beads. The PIV algorithm splits each frame into a large number of integration areas called windows and then calculates a displacement vector for each window using signal processing and auto-correlation/cross-correlation techniques. This is converted to a velocity using the time between each image frame and the physical size of each pixel on the camera [28]. Using the PIVlab application in MATLAB [29], velocity magnitudes, shear rates, and strain rates were calculated along lines transversal and radial to the needle geometry. These values were calibrated using the scale bar of the image and the image acquisition rate. In addition, heat maps were generated illustrating the velocity magnitude as a function of space to identify areas of most impact. Finally, tangential velocities were calculated at specific locations relative to the needle tip and were converted into displacement for each frame to model the mechanics of tissue over time.

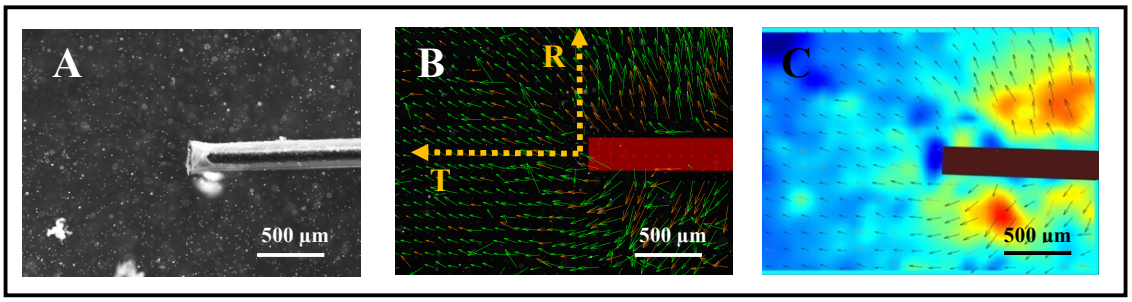

Figure 2.1: *(a) Agarose brain phantom embedded with fluorescent beads and a needle for infusion (b) Velocity vectors generated from PIV analysis transversal (T) and radial (R) to needle geometry (c) Heat maps derived from velocity magnitudes. Sample images obtained from 500 µL/min trials.*

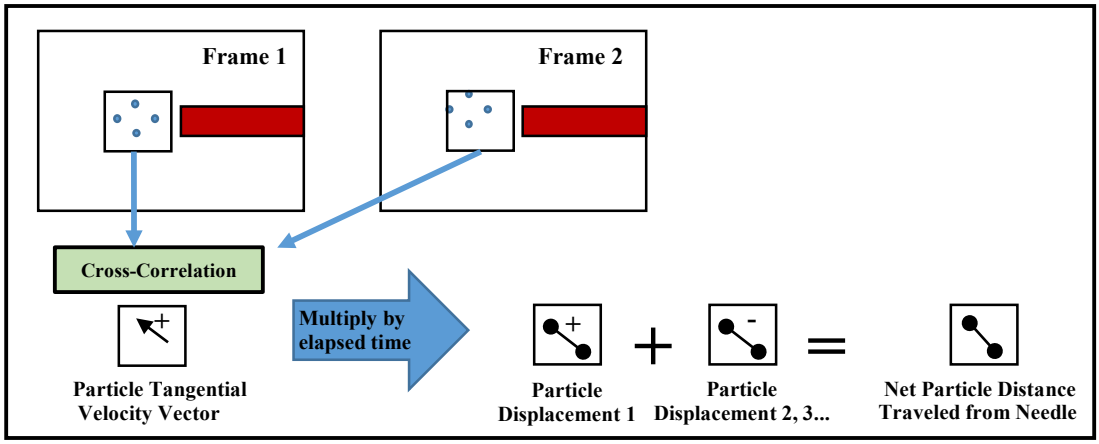

Figure 2.2: *Schematic illustrating how tangential velocity can be converted to net displacement from the needle tip to model deformation over time.*

2.2.3: CED Backflow Studies

Matrix deformation results are compared to preliminary CED backflow studies that have been previously conducted for similarities in drug distribution behavior. For these studies, agarose brain phantoms were made into modified well plates and bromophenol blue dye was infused to track the fluid path for selected flow rates. Images were taken through the course of infusion and the percent of backflow was calculated using image processing on ImageJ to correlate the intensity of the dye in front and behind the needle tip to the volume of dye. This preliminary work was done courtesy of Dr. Sy's 2017 senior design team.

2.3 Results

2.3.1: Magnitudes of Matrix Deformation

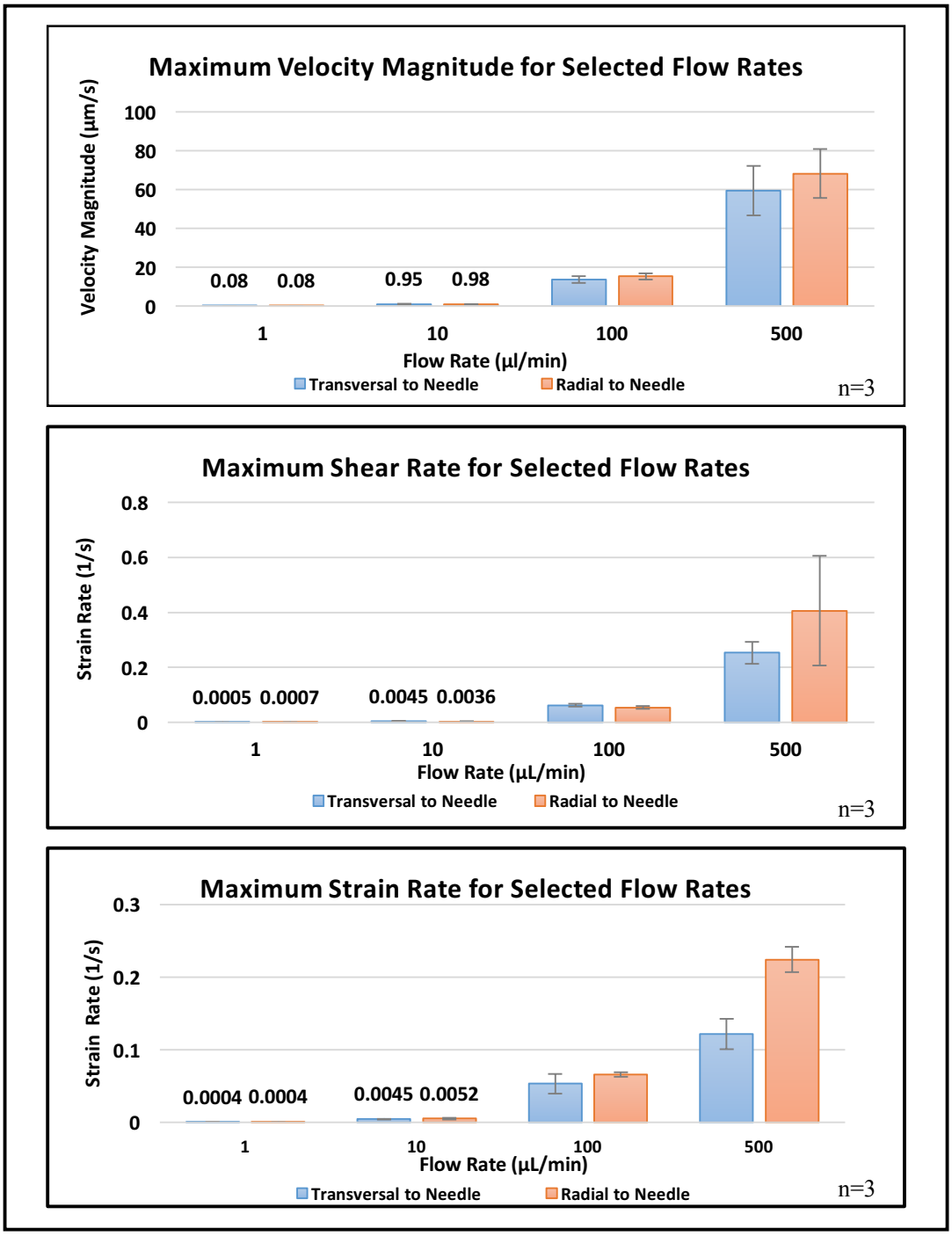

Figure 2.3: *Maximum velocity magnitudes, shear rates, and strain rates calculated at the onsite of infusion in both directions transversal and radial to needle geometry for the selected flow rates. N=3.*

2.3.2: Deformation as a Function of Distance from the Needle Geometry

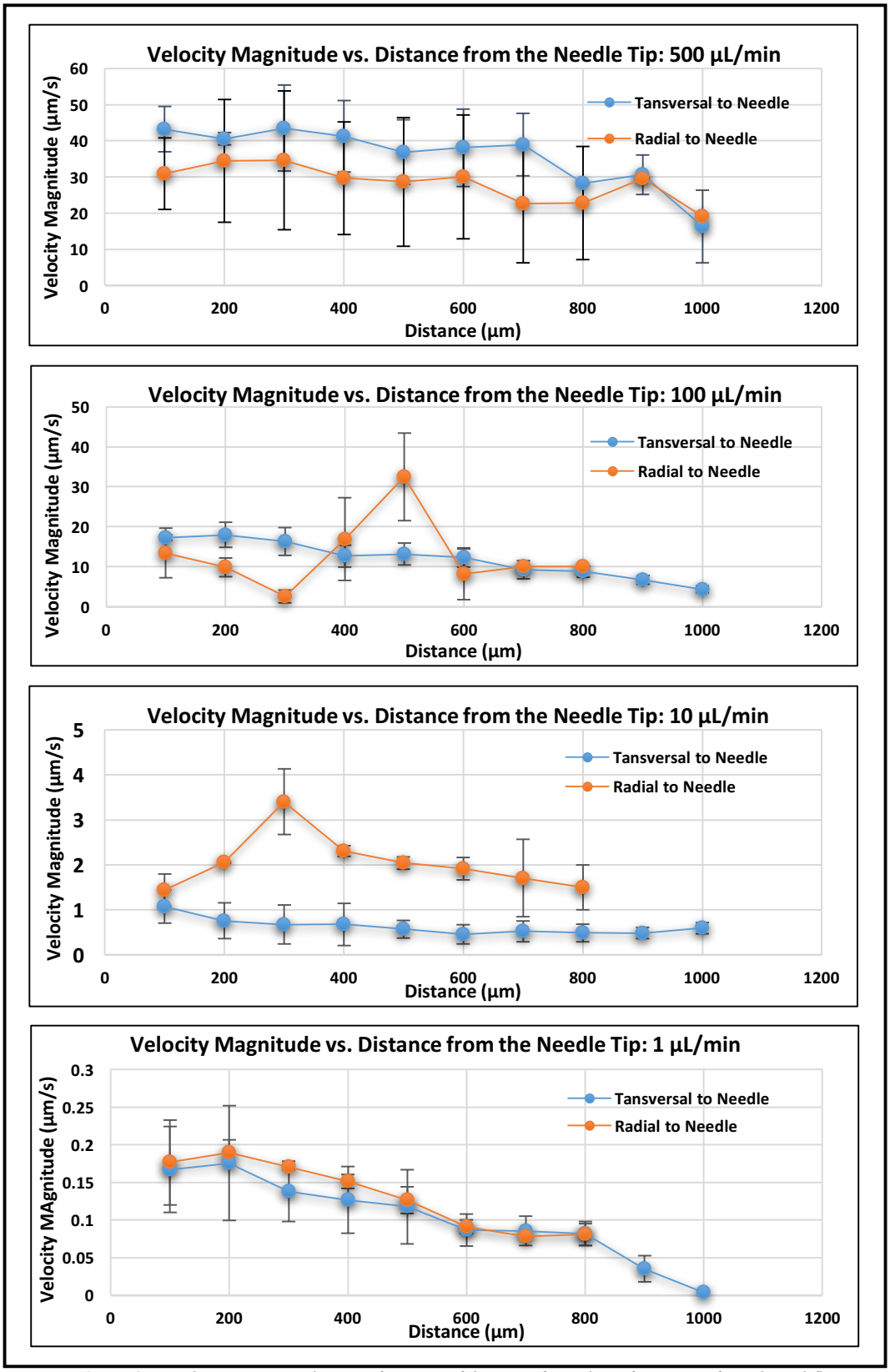

Figure 2.4: *Velocity magnitudes as a function of distance from the infusion site for selected flow rates along lines both transversal and radial to needle geometry. N=3.*

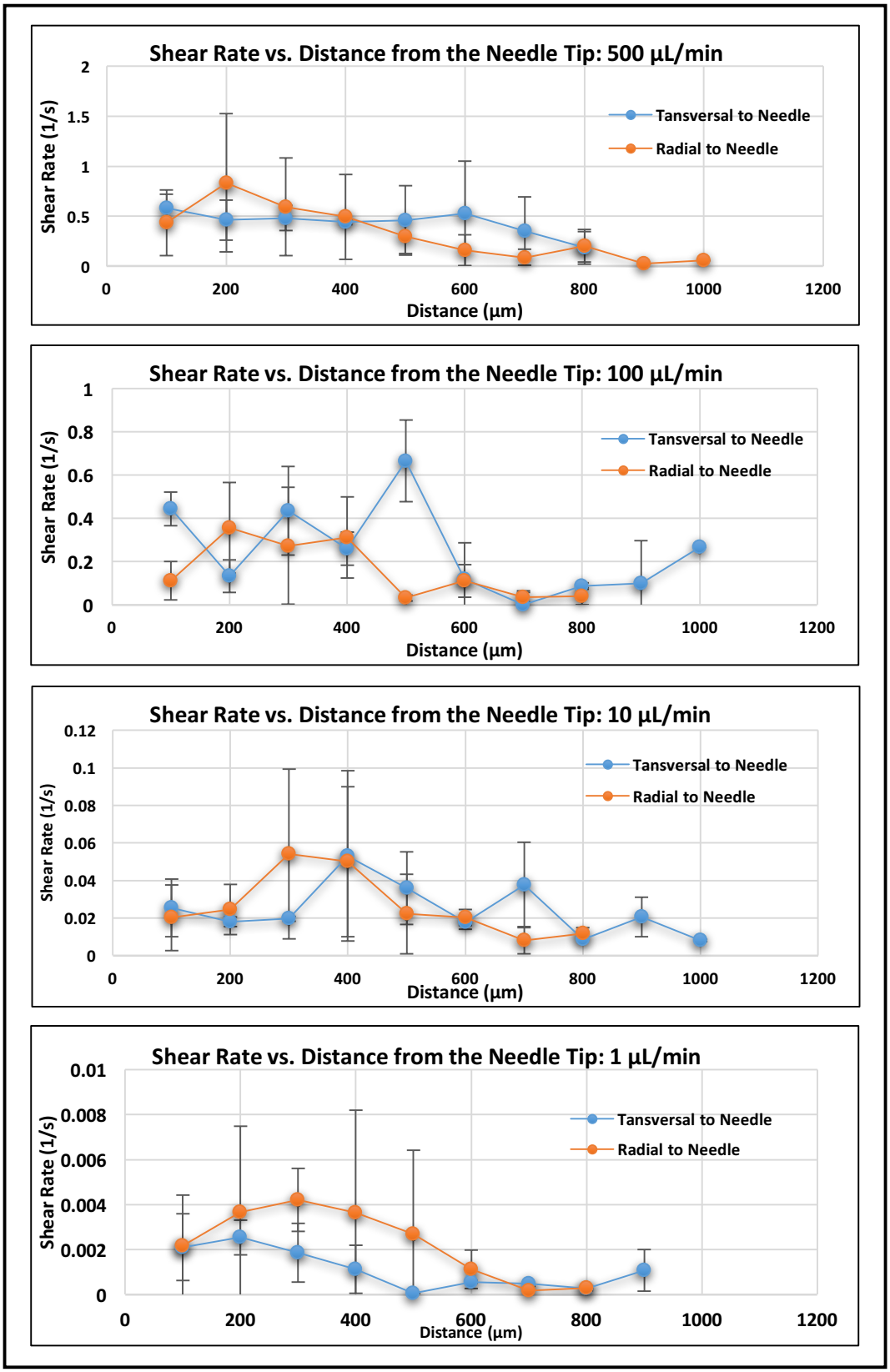

***Figure 2.5**: Shear rate as a function of distance from the infusion site for selected flow rates in both directions transversal and radial to needle geometry for the selected flow rates. N=3.*

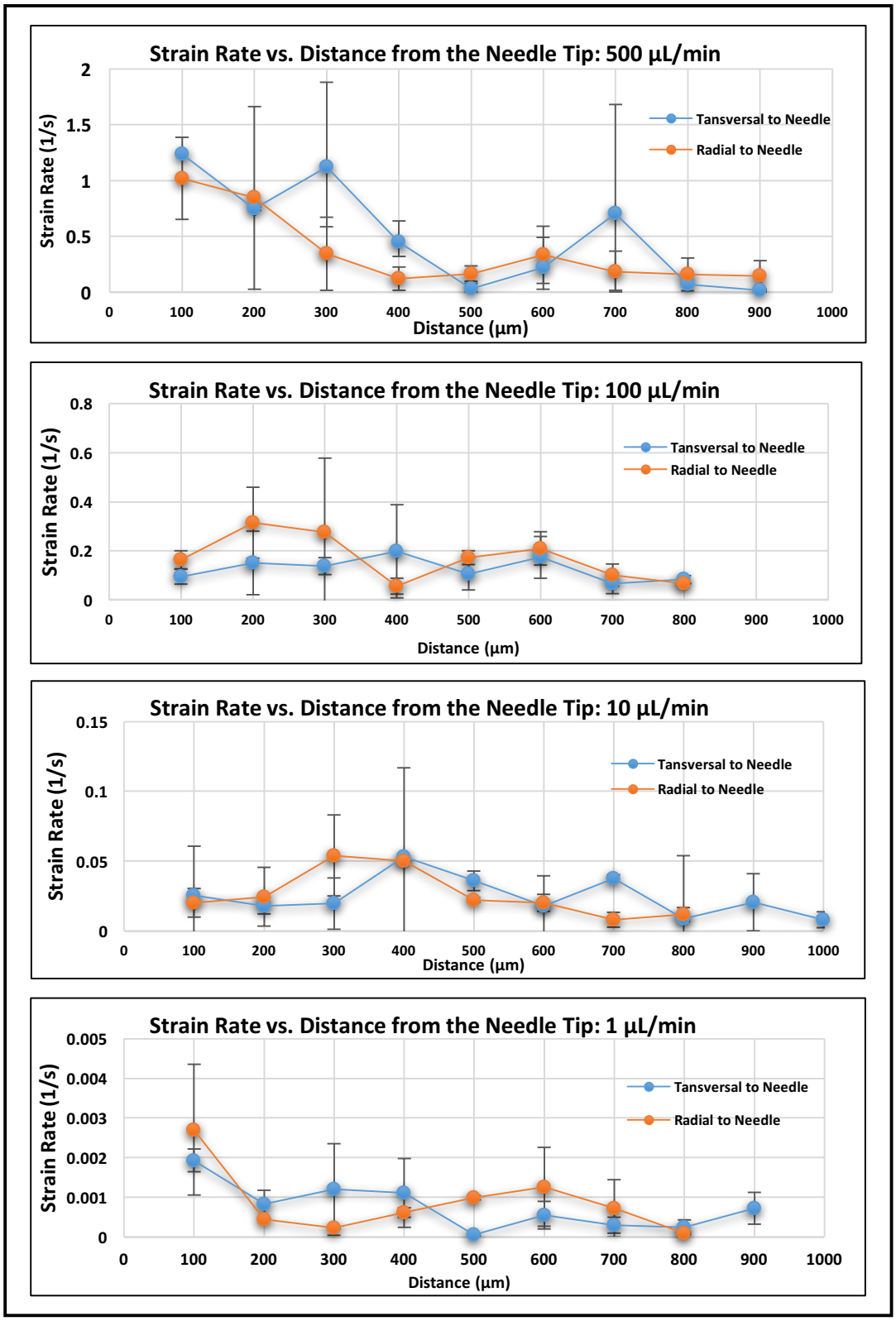

Figure 2.6: *Strain rate as a function of distance from the infusion site for selected flow rates in in both directions transversal and radial to needle geometry for the selected flow rates. N=3.*

2.3.3: Deformation over Time

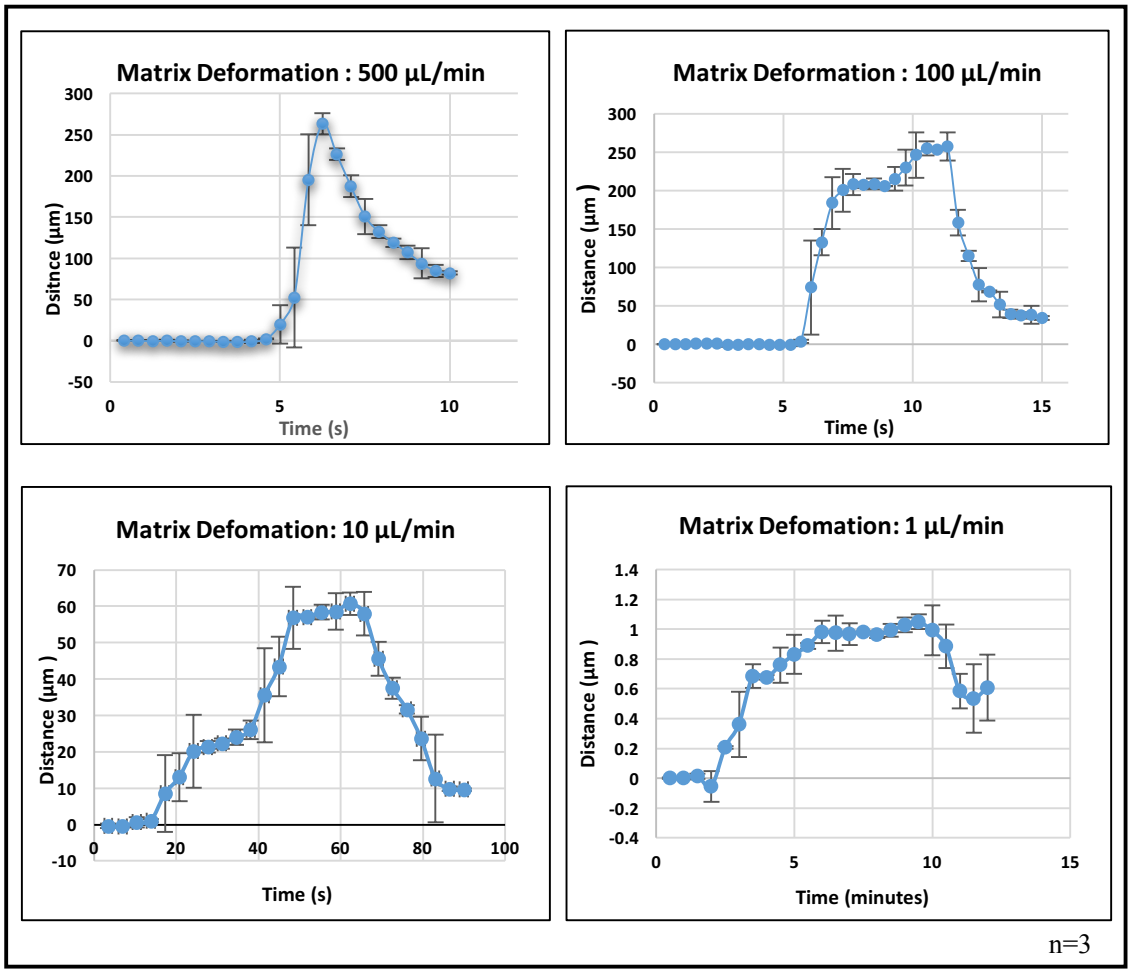

Figure 2.7: *Deformation as a function of time 100 µm transversal from the infusion site for selected flow rates. Infusion begins approximately after 5 seconds for 500 µL/min and 100 µL/min, 20 seconds after for 10 µL/min and 1 minute for 1µL/min. N=3.*

2.3.3: Particle Image Velocimetry- Spatial Analysis of Matrix Deformation

A. 500 µL/min

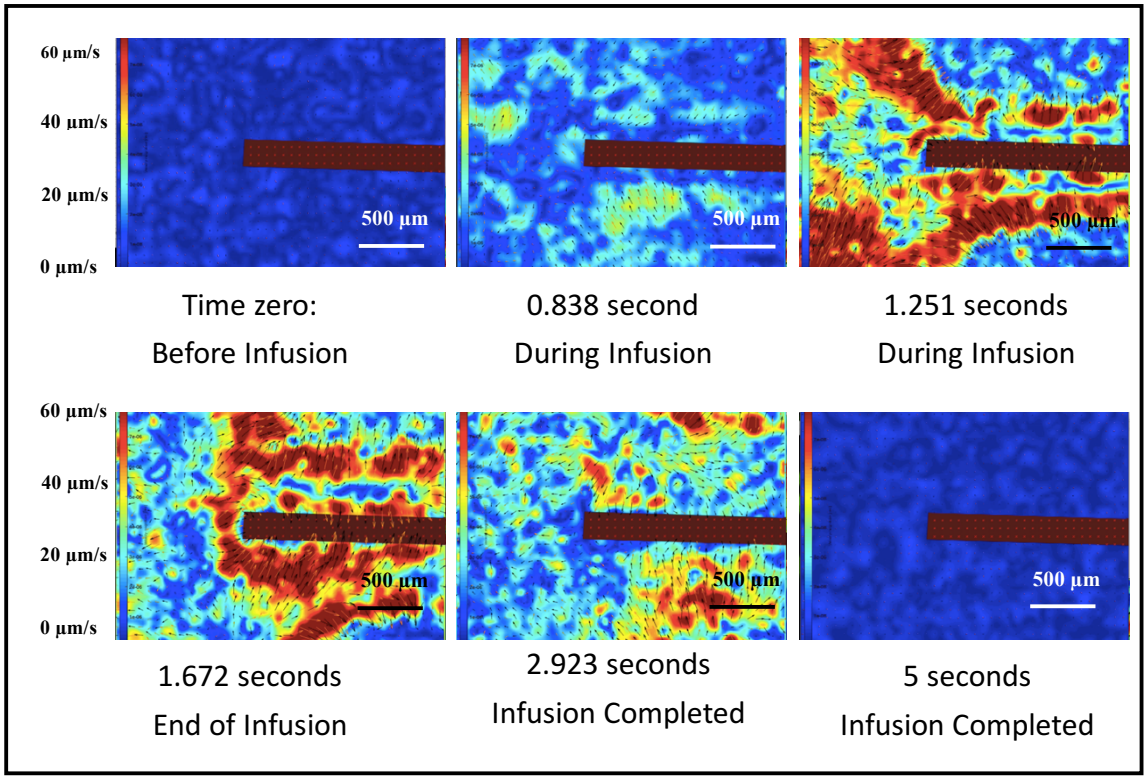

Figure 2.8: *Heat map illustrating velocity magnitudes at selected points of time as the matrix expands and relaxes for the 500 µL/min infusion rate. Three trials analyzed in total; one representative trial shown above.*

B. 100 µL/min

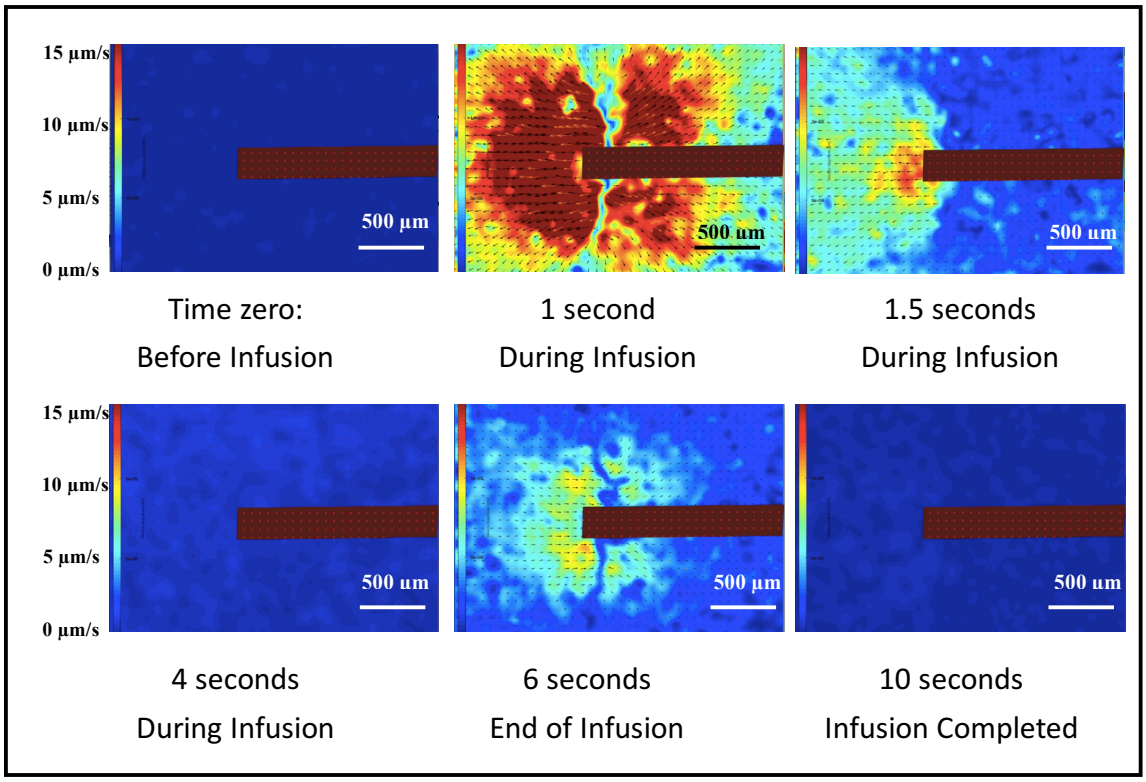

Figure 2.9: *Heat map illustrating velocity magnitudes at selected points of time as the matrix expands and relaxes for the 100 µL/min infusion rate. Three trials analyzed in total; one representative trial shown above.*

C. 10 µL/min

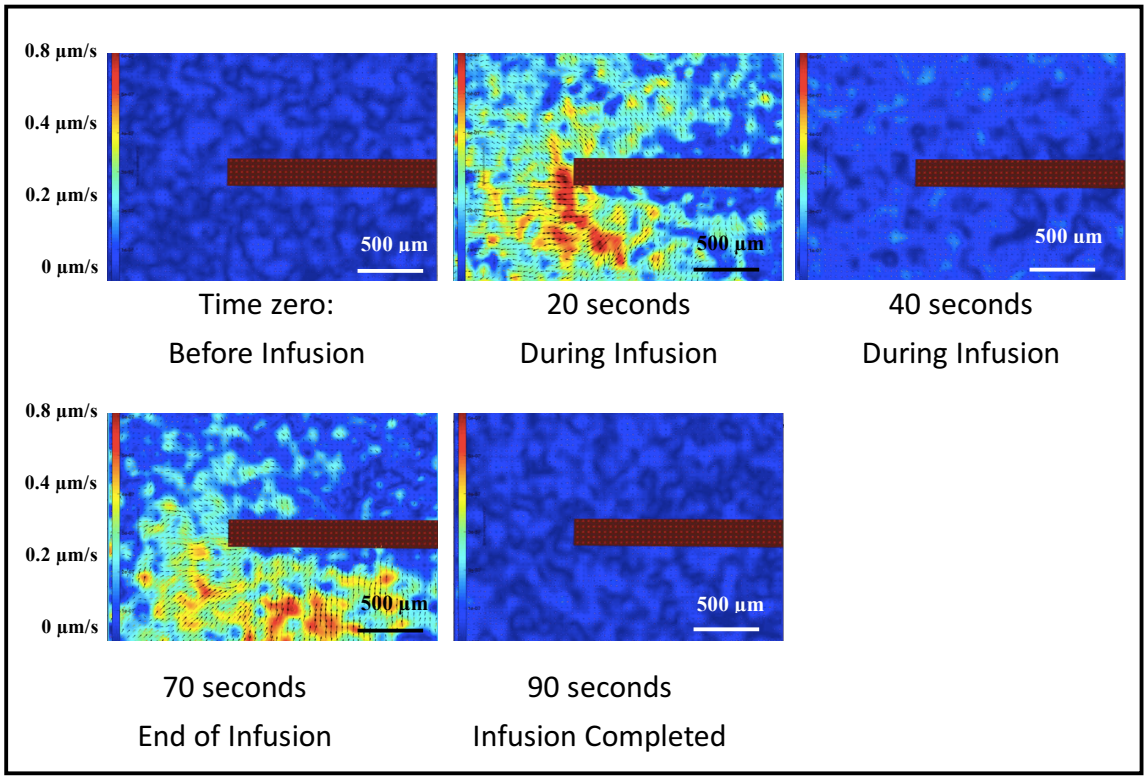

Figure 2.10: *Heat map illustrating velocity magnitudes at selected points of time as the matrix expands and relaxes for the 10 µL/min infusion rate. Three trials analyzed in total; one representative trial shown above.*

D. 1 µL/min

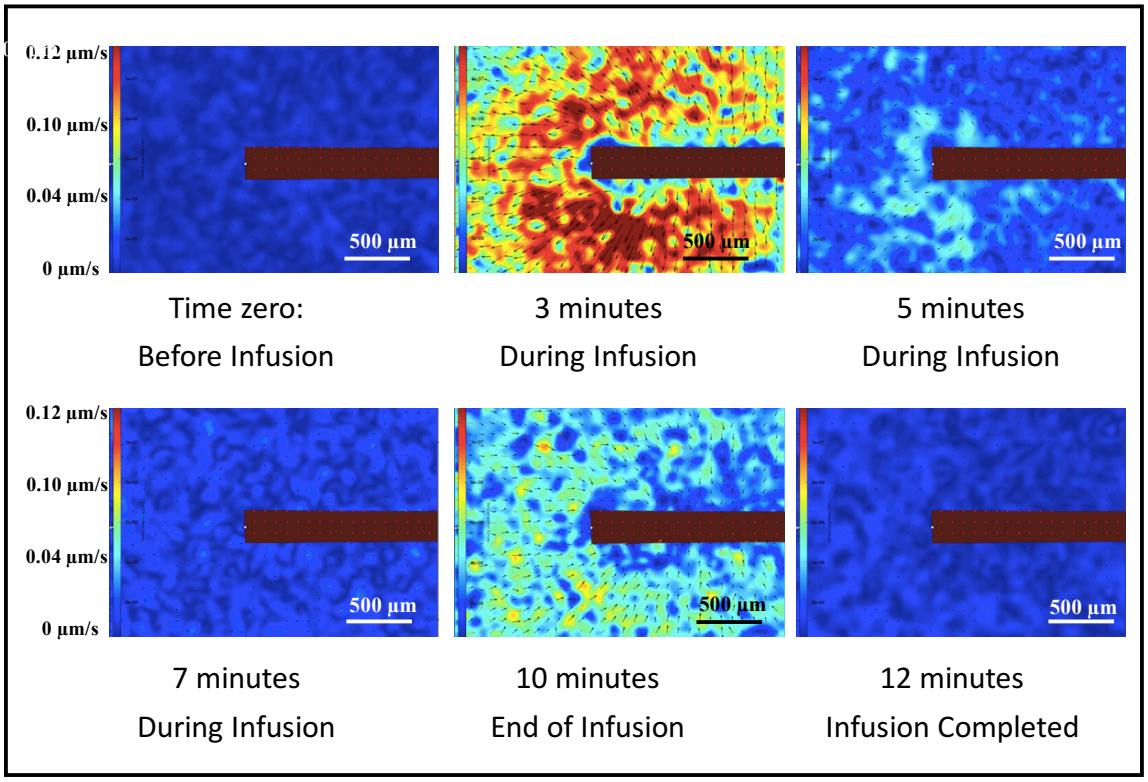

Figure 2.11: *Heat map illustrating velocity magnitudes at selected points of time as the matrix expands and relaxes for the 1 µL/min infusion rate. Three trials analyzed in total; one representative trial shown above.*

2.3.3: Backflow Analysis

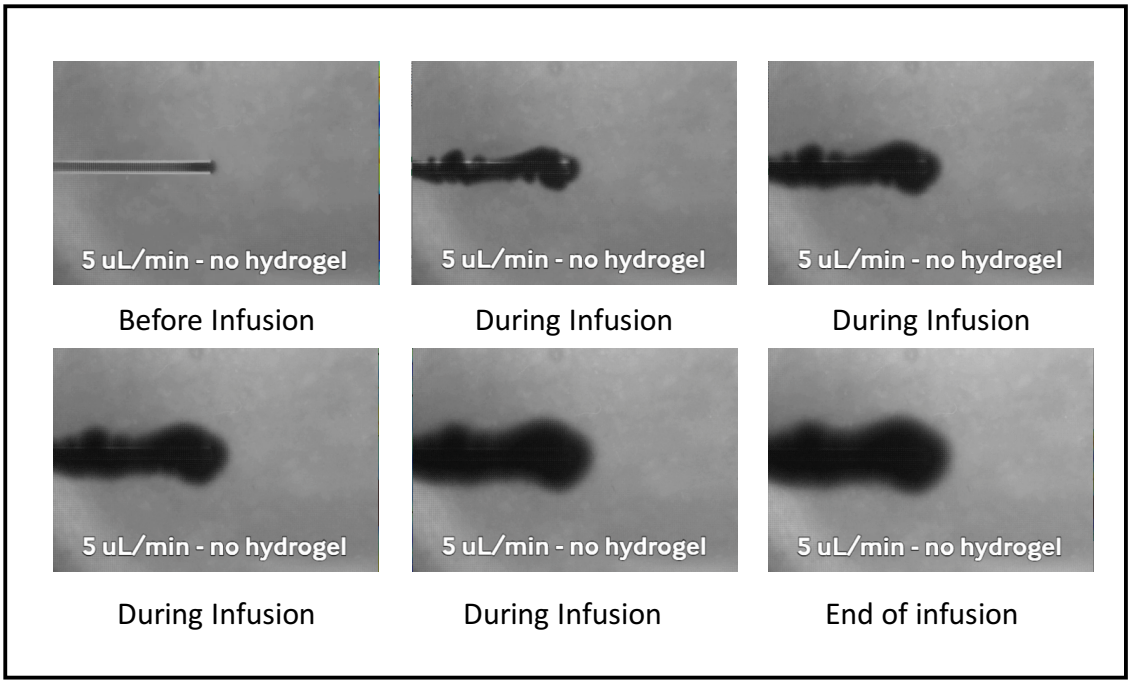

Figure 2.12: *CED backflow study at 5 µL/min showing the evolution of backflow at different time points during the infusion from bromophenol blue dye in a 0.6% agarose brain phantom.*

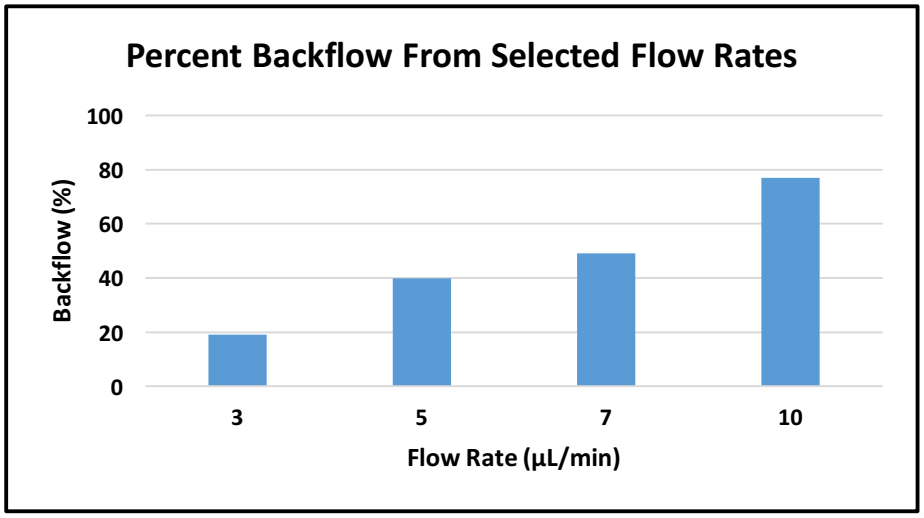

Figure 2.13: *Preliminary CED backflow study at various flow rates which suggests backflow is proportional to the infusion rate, similar to what is seen in literature [11].*

2.4 Discussion

Figure 2.3 highlights the maximum velocity magnitude, stress rate, and strain rate calculated at the onsite of infusion for the selected flow rates using particle image velocimetry. PIV analysis appears to be successful in detecting low-magnitude deformation from fluid shear. In all cases, the maximum deformation is within 1 mm from the site of infusion. The velocity magnitude, shear rate, and strain rate from matrix deformation are proportional to flow rate. We also see that as the flow rate is increase, the area of tissue affected is also proportional. Looking at **Figures 2.4, 2.5, and 2.6,** we observe that velocity magnitude, shear rate, and strain rate decrease as function of distance from the needle tip along lines both transversal and radial to the needle geometry. Magnitudes of transversal and radial behavior are similar. However, as the flow rate is deceased, there is a change in behavior radial to the needle tip that is not present transversal to the needle geometry. There is a spike in all components that shifts closer to the needle as the flow rate is decreased. This can perhaps be explained using previous backflow studies that have been conducted **(Figure 2.12 & Figure 2.13)** which suggest that as flow rate is decreased, drug distribution becomes more radial as there is less backflow, indicating why we see a difference in behavior radial to the needle tip. This phenomenon is again reinforced through heat maps generated from PIV which allow for spatial analysis of matrix deformation **(Figures 2.7-2.11)**. Here, we can clearly see both matrix expansion and relaxation from the needle tip for all flow rates. It is apparent that backflow plays a prominent role in influencing tissue deformation from fluid shear. For slower infusion rates, the radius of tissue deformation from the infusion site is higher whereas with the higher infusion rates, deformation is narrowed to a smaller area and high magnitudes of velocity are found back

against the needle. This response is again supported by the backflow studies have shown increased levels of backflow with increased flow rate **(Figure 2.12 and 2.13)**. Lastly, we quantify matrix deformation as a function of time **(Figure 2.7)**. Deformation over time shows viscoelastic behavior: fluid shear serves as a constant applied stress that results in a time-dependent increase in strain, or creep. When the infusion is done, the applied force is removed and the matrix relaxes gradually to a residual strain. Comparing the different flow rates, it is apparent that creep and stress relaxation takes longer with slower infusion rates.

These findings allow us to make predictions on potential implications of fluid shear on immune response from brain tissue. In literature we have seen that strain rates as high as $20s^{-1}$ are needed to cause significant reduction in glial cell viability [30]. However, low magnitude strains (1-5%) can activate glial cells and cause up-regulation of inflammation markers associated with glial scarring [5]. PIV analysis of micromotion has revealed that micromotion can cause matrix displacements within a magnitude of 100 μm and shear strain within a magnitude of .15. Both of these magnitudes are observed within a distance of 200 μm from the device [18]. This mechanical behavior and these magnitudes are comparable to what we see for flow rates 10 μL/min and higher. The same study has shown that these magnitudes are capable of inducing glial reactivity [18]. This suggests that there is potential for us to see glial cell activation for infusion rates on the high end of the CED range as well as extreme cases. It is important to note that for the micromotion studies, strains were applied for long durations of time (hours to weeks) whereas in our case the mechanical behavior to fluid shear is an impulse response. Additionally, the prominence of backflow which is not involved in micromotion may affect the area of cells affected. These two factors may affect the biological implications and will need to be explored. All

in all, these results illustrate that PIV analysis can provide a simple method for in depth characterization of tissue deformation from fluid shear. This mechanical behavior can potentially have a direct correlation with inflammation response similar to what we have seen in literature which we explore in the next chapter.

CHAPTER 3: BULK ANALYSIS OF TNF-α -FOR QUANTIFICATION OF BRAIN INFLAMMATION FROM FLUID SHEAR

3.1 Motivation

As discussed in Section 1.4.2, many studies support the notion that low magnitude shear or strain from brain implants can cause mechanotransduction of glial cells. We attempt to translate this type of study to the investigation of CED devices to better understand the effects of flow alone on cell activation to explore any potential biological constraints that need to be considered for the development and clinical use of CED devices. We hypothesize that fluid shear can cause activation of surrounding glial cells near the infusion site, as similarly seen with other brain implants, posing biological restrictions. In this section, we develop a simplified cellular environment to test this phenomenon and conduct infusion experiments to measure a candidate biomarker that can indicate any increased levels of inflammation.

3.2 Experimental Design & Rationale

3.2.1 Development and Viability of the in Vitro 3D Cell Model

The development of the *in vitro* 3D cell model requires selecting an appropriate cell line and an extracellular matrix. Here we will discuss the rationale behind the materials chosen and the methods used to develop and test the 3D cell model for viability to ensure that we can achieve brain density and confirm that the cells will be viable for the duration of the experiments.

A. C8 B4 Mouse Microglial Cell Line

Microglia, as discussed in Section 1.4, are the most prominent immune cells found in the central nervous system. They play a critical role in immune surveillance and have been used in previous glial scar models, thus making them an ideal cell type for this preliminary study. They can get activated and turn phagocytic when exposed to different stimulus and as a result secret many biological signals such as cytokines and chemokines. The particular cell line selected for this study is C8-B4, a spontaneous immortalized mouse microglial cell line [31]. This cell line has been previously used for various types of immunology studies. Zuo, et al. have used C8-B4 microglia to study the anti-inflammatory response of the molecule resveratrol and Ooi, et al. investigated the use of isoflurane and morphine preconditioning to reduce microglial activation and injury by LPS [32,33]. The results of these studies have shown that these cells are responsive to different kinds of stimuli and have the potential to release various cytokines and chemokines when activated. Thus C8-B4 microglia can serve as a simplified model of brain parenchyma and can elucidate molecular responses from inflammation.

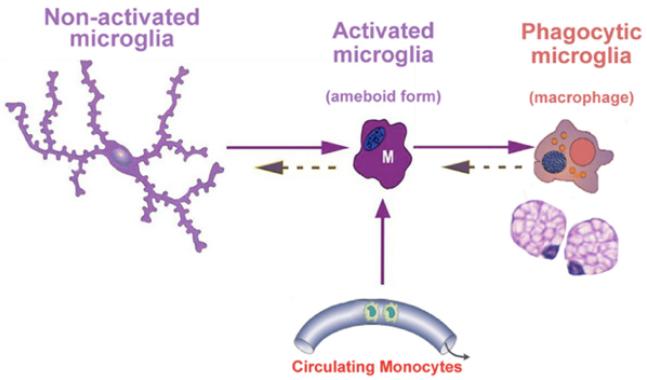

***Figure 3.1**: Schematic illustrating the activation of microglia as a response to stimuli [23].*

B. Matrigel as the Basement Membrane

As discussed in Section 1.4, many types of extracellular matrix materials have been explored for the development of 3D glial cultures, one of which is Matrigel. Matrigel is an extracellular matrix that is found in all epithelial and endothelial cells. It serves many functions, some of which include maintaining tissue integrity and specificity, providing a barrier to cells and molecules, separating tissue types, and transducing mechanical signals. The major components of Matrigel are laminin, collagen, proteoglycans, growth factors, and proteases. The amount and type of these components dependent on the stage of development and tissue type from which it is derived. These components from specific interactions with each other which together form an organized matrix [34]. Previous 3D gel models have used collagen cultures for encapsulation of glial cells [35,36]. However, these models are limited because there is no collagen in the brain extracellular matrix (ECM) and thus may not be the best representation of the brain parenchyma and can ultimately impact cell behavior. However, the brain does contain laminin, one of the major components of Matrigel (nearly 60%), and therefore can be better suitable as a brain mimetic material [37]. A study by Searson, et al. compares collagen, hyaluronic acid (HA), collagen+HA mixed, and collagen+HA+Matrigel mixed gels and have found that this combination has allowed for endothelial cell compatibility and have shown that glial cells are in in a more quiescent state [22]. The results of these studies show further promise that Matrigel may be a more accurate ECM for development of the 3D cellular microenvironment compared to other readily available options.

C. Selected Parameters & Methods:

C8-B4 microglia were seeded at a concentration of 3.75 X 10^6 cells/mL in 24 well plates. This seeding density was chosen as it has been shown to maximize viability of neural cultures [30]. Matrigel at a concentration of 4.2 mg/mL was chosen based on previous preliminary rheology studies that suggest similar mechanical properties to brain tissue. A live/dead assay was used to assess viability and quantified manually using ImageJ.

3.2.2 *In Vitro* Infusion Experiment Setup

The microenvironment and setup used for the infusion experiments are shown in **Figure 3.2 and 3.3** respectively. A programmable syringe is used to infuse media using the same flow rates as used for the mechanical studies: 1 μL/min, 10 μL/min, 100 μL/min, and 500 μL/min. Table 3.1 describes the three experiments performed. Experiment #1 was conducted by keeping the volume constant and changing the flow rate and infusion duration whereas Experiment #2 and Experiment #3 were conducted with the flow rate held constant at a low value used clinically in CED (10μL/min) and a high value above standard CED rates (100 μL/min) respectively. This is to differentiate between effects of changing the flow rate and time of duration versus effects of changing the duration and volume of infusion. For these experiments, media was replaced immediately after infusion to normalize volume and ensure constant dilution of cytokines that may be secreted. Experiments were conducted in the cell culture incubator (37 ˚C, 5% CO_2) and left for 6 hours in order to ensure sufficient time for cell activation. Lipopolysaccharide (LPS) is a commonly used agent to induce inflammation and used in many cell activation studies.

LPS-treated cultures serve as a positive control whereas cells with no treatment or infusion are the negative control.

Figure 3.2: *The microenvironment is shown above and* is *comprised of C8-B4 microglia encapsulated in 3D Matrigel cultures in a modified well plate that facilitates the insertion of a needle for infusion and has been sterilized with ethylene oxide.*

Figure 3.3: *Experiment setup is shown here. Infusion experiments are conducting with a syringe pump is placed into a cell culture incubator at 37˚C and 5% CO_2.*

Table 3.2: *Infusion parameters tested for each experiment. In Experiment #1, volume is kept constant while the infusion rate and duration are changed. In Experiment #2 and #3, infusion rate is kept constant at 10µL/min and 100 µL/min respectively while infusion volume and duration are changed.*

Experiment #1: Constant Volume- Varying Flow Rate & Infusion Duration

Flow Rate (µL/min)	Infusion Duration	Volume (µL)
1	10 minutes	10
10	1 minute	10
100	6 seconds	10
500	1.2 seconds	10

Experiment #2: Constant Flow Rate (10 µL/min)- Varying Infusion Duration & Volume

Flow Rate (µL/min)	Infusion Duration	Volume (µL)
10	1 minute	10
10	10 minutes	100
10	30 minutes	300

Experiment #3: Constant Flow Rate (100 µL/min)- Varying Infusion Duration & Volume

Flow Rate (µL/min)	Infusion Duration	Volume (µL)
100	1 minute	10
100	5 minutes	500
100	10 minutes	1000

3.2.3 Bulk Quantification of Cell Activation & Inflammation Response

Inflammation can cause activation of glial cells in the brain, resulting in the signal transduction of many molecular pathways. One such pathway that plays a prominent function in inflammation, immune response, and cell survival is the nuclear factor kappa-light-chain-enhancer of activated B cells (NF-kB) pathway. There is an abundance of NF-kB transcription factors found in the brain and stimulation of microglia can activates the IκB kinase complex, causing the release of different types of pro-inflammatory cytokines and chemokines as shown in **Figure 3.3** [38,39]. Some of these biomarkers include Tumor Necrosis Factor Alpha (TNF-α), Interleukin-1 Beta (IL-1ß), Transforming Growth Factor Beta (TGF-ß), Interleukin-6 (IL-6), and nitric oxide (NO). There has been a clear trend established between cytokine production and glial inflammation indicating that elevations in the production of these cytokines can be a good indicator for inflammation. In order to identify and quantify the cell activation as a response to infusion for this study, TNF-α was selected as the candidate biomarker and evaluated using an Enzyme-linked Immunosorbent Assay (ELISA).

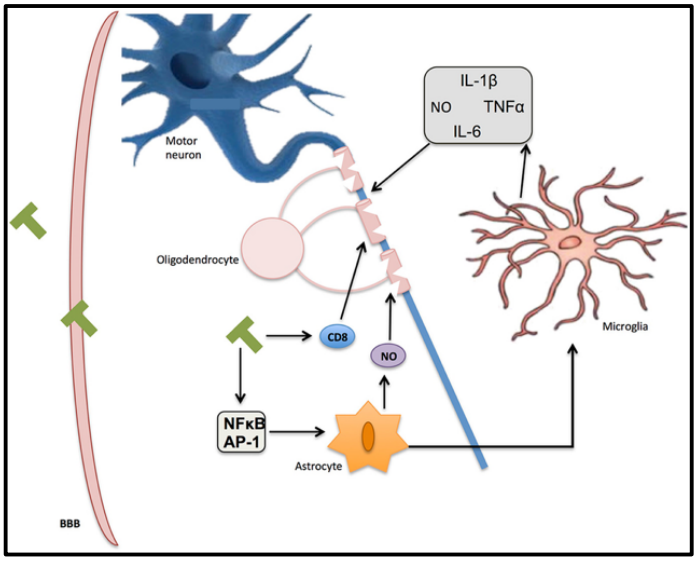

***Figure 3.4**: The NF-kB molecular pathway illustrating microglial activation following a stimulus and the production of various biomarkers [39]*

3.3 Results

3.3.1: Live/Dead Assay

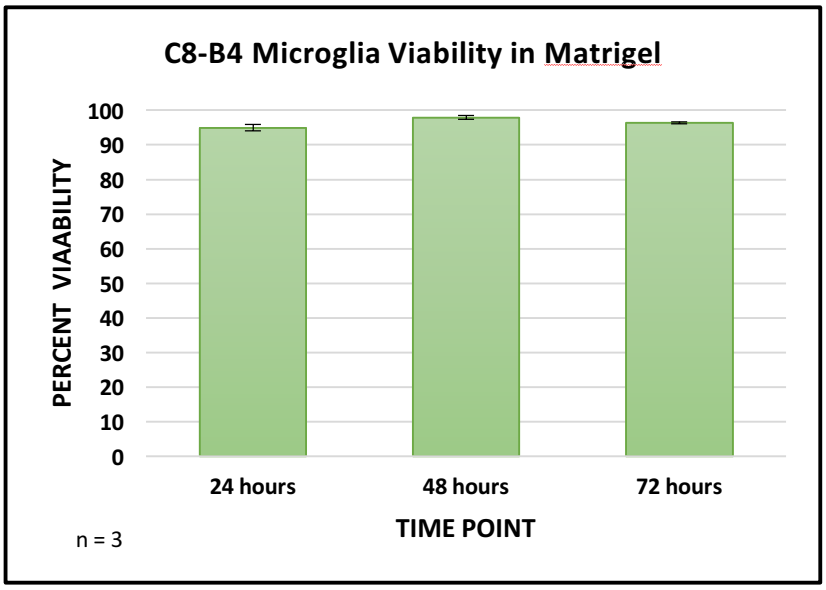

Figure 4.5: *Results indicate that C8 B4 Microglia shows that cells are viable (>90 % viability) for at least 72 hours. Three samples have been analyzed for each time point.*

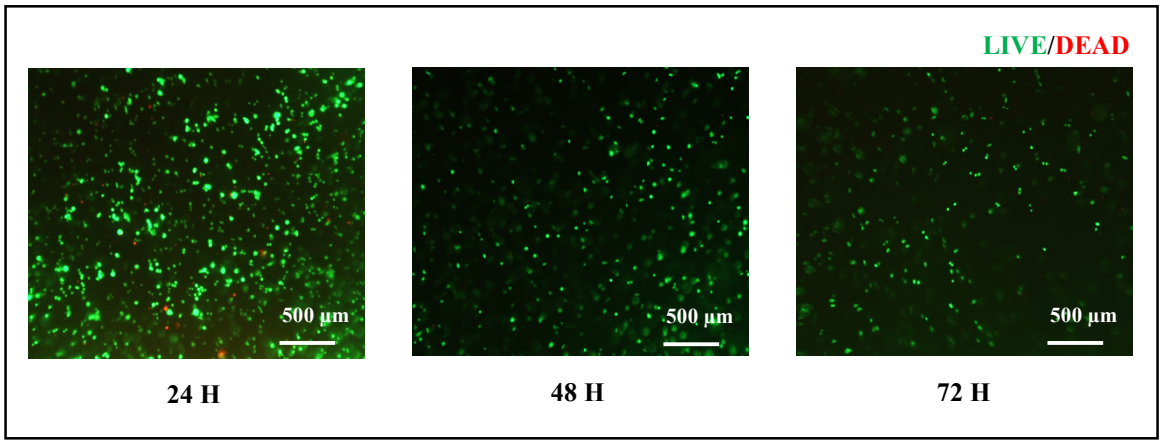

Figure 3.6: *Representative images at time points 24 hours, 48 hours, and 72 hours illustrating viability of C8-B4 microglia in Matrigel. Images taken at 40X for three different areas per sample. N=3.*

3.2.2: Infusion Experiments Results

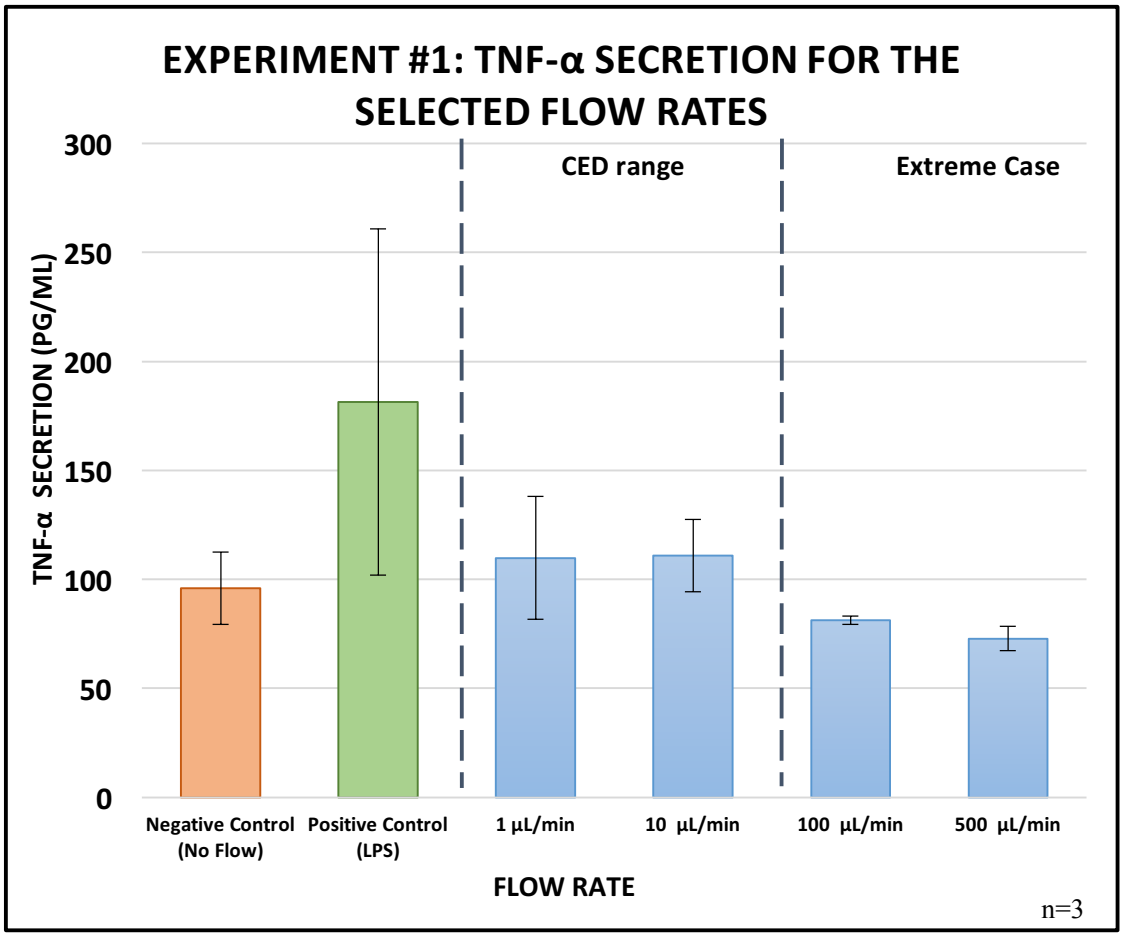

Figure 3.7: *TNF-α secretion for the selected flow rates. Three replicates per flow rate.*

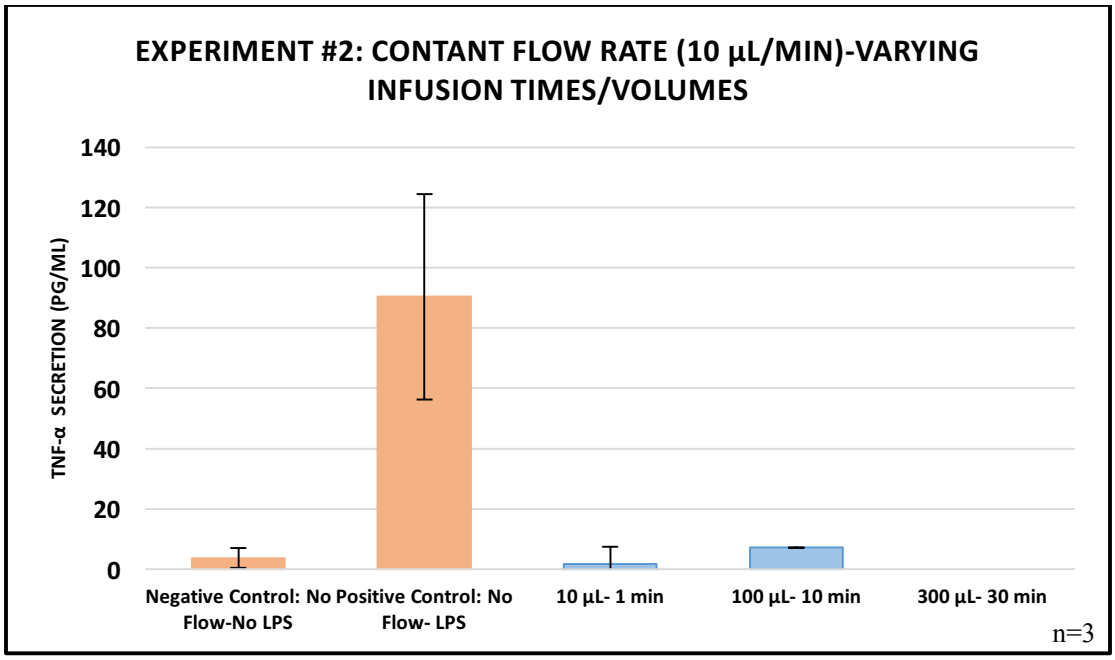

Figure 3.8: *TNF-α secretion at 10 µL/min for the selected infusion times/volumes. Three replicates per flow rate.*

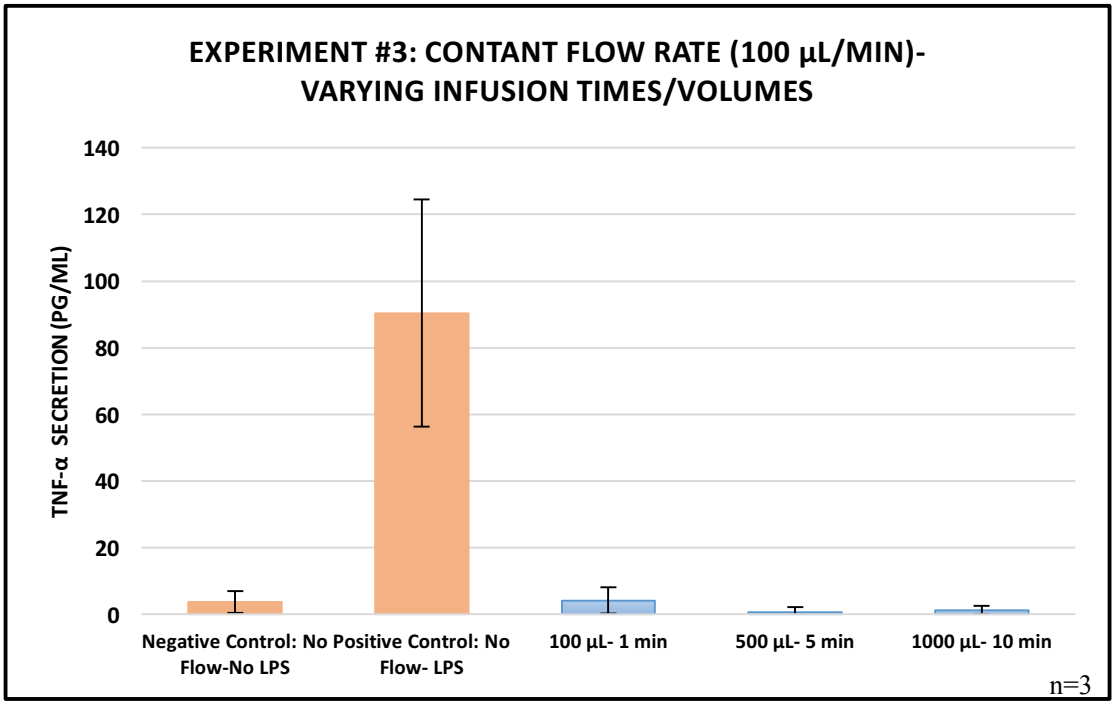

Figure 3.9: *TNF-α secretion at 10 µL/min for the selected infusion times/volumes. Three replicates per flow rate.*

3.3 Discussion

Figure 3.5 and **3.6** highlight the live/dead assay results from each time point which show that the C8-B4 mouse microglia are viable at the selected seeding density for at least 72 hours. This ensures that majority of the cells are live for the duration of the infusion experiments and suggests that Matrigel is viable option for development of the 3D glial microenvironment. In Experiment #1 **(Figure 3.7)**, the volume of infusion was kept constant while the flow rate and infusion time was varied. Although we see a minor inverse trend in TNF-α secretion as the flow rates are decreased and the time of infusion is increased, this is not a significant increase in TNF-α secretion in comparison to the positive control. All samples induced with fluid shear appear to be more similar to the negative control indicating merely basal express of TNF-α. However, due to the slight inverse trend, we explored the possibility that perhaps inflammation response can be proportional to infusion time as opposed to infusion rate. This was investigated in experiments #2 and #3 where the flow rate was kept constant either at a low CED value of 10 μL/min or a high value of 100 μL/min. However, again we do not see a significant secretion of TNF-α as seen with the positive control and the levels are much more similar to the negative control **(Figure 3.8 & Figure 3.9)**.

The results from this study can perhaps be explained through the tissue mechanics studies from Chapter 2. We've seen that from the mechanical studies that radius of tissue deformation is quite small (<1 mm) due to matrix resistance and backflow. Backflow causes the areas of deformation to be along the track of the needle rather than radially outward from the needle tip, reducing the area of cells that are affected by flow. As a result, it is possible that the region of inflammation is too minuscule to be detected by a

bulk quantification method such as an ELISA or that the cells do not produce sufficient cytokine to activate positive feedback in the cell signaling cascade. Therefore, a method that can provide more local resolution of inflammation from fluid shear may be a more effective technique to use in conjunction with bulk analysis.

CHAPTER 4: BREFELDIN A FOR SPATIAL ANALYSIS OF BRAIN INFLAMMATION FROM FLUID SHEAR

4.1 Motivation

Although quantifying the extent of microglial activation using an ELISA, as done in Chapter 3, can provide valuable information in regard to inflammation response from fluid shear, because it is a bulk quantification method, it may not be as reflective of local immune response. If the area of impact from fluid shear is small, as we've seen to be the case from the tissue mechanics in Chapter 2, the immune response can appear miniscule with this kind of bulk analysis. For this reason, spatial analysis of cell activation using fluorescent cytochemistry can be beneficial by providing visual insight into cell activation locally near the infusion site. This section will discuss a study that has been conducted with the secretory inhibitor Brefeldin A (BFA) to see if it can be a viable method for developing a staining protocol that can eventually be used in conjunction with an ELISA for spatial analysis to determine the effects of fluid shear from CED devices on local cell activation and inflammation.

4.2 Experimental Design & Rationale

4.2.1: Introduction to Brefeldin A

Immunofluorescence allows for direct visual analysis of which cells express a specific biomarker and is based around the notion that we can use the specificity of antibodies to their antigen as an advantage to link fluorescent dyes to specific biomarker

targets in a cell. This allows for staining of the biomarker of interest and can be imaged using fluorescent microscopy.

One of the challenges in developing an immunofluorescence protocol is ensuring that the biomarker of interest is retained within the cell to bind to the fluorescently-linked secondary antibody and emit a strong fluorescent signal for imaging. If the protein is already secreted from the cell before the staining process, this can result in a weak signal and the expression of this protein within the cell may be lost. There is a trade off between increasing fluorescent signal from the cell versus seeing a localized signal that needs to be explored. This issue can potentially be overcome by treating the cultures with a secretory inhibitor such as Brefeldin A. Brefeldin A (BFA) is a lactone antiviral that can be derived from a variety of fungi and its mechanism of action involves preventing the formation and transport of secretory vesicles from the Endoplasmic Reticulum to the Golgi apparatus, as shown in **Figure 4.1** [40]. This causes a temporary retention of unprocessed secretory proteins within the cell. Applying this knowledge to our study, if the microglial cultures are treated with BFA at the optimal time, BFA can prevent secretion of certain cytokines that follow this secretory pathway, one of which is TNF-α. The timing of BFA treatment is critical to retain the cytokine within the cell and emit a strong signal for imaging and balance the positive feedback of signal to see a localized response. It is also specific to cell type and the cytokine selected. Therefore, an optimization experiment is conducted to see if BFA treatment is a viable method for spatial analysis of inflammation and if so, determine the optimal time to treat the glial cultures with BFA.

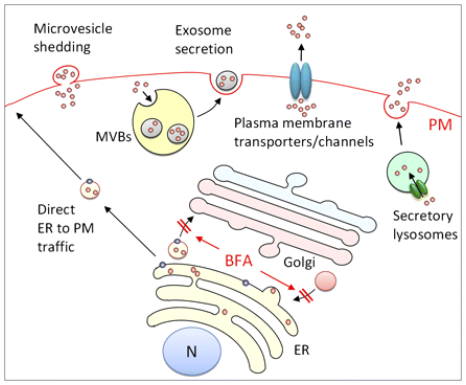

Figure 4.1: *Brefeldin A Mechanism of Action [41].*

4.2.2: Selected Methods & Parameters

C8-B4 microglial cells were seeded in 2D monolayer cultures and LPS was used as a stimulus to induce cell activation for all samples. The study was conducted by treating the cultures with BFA at different time points and quantifying elevations in TNF-α using both an ELISA and immunofluorescence. The ELISA will allow us to quantify the amount of TNF-α that has been secreted by the cells at the specific time point where as the fluorescence results from the staining will allow us to quantify the amount of TNF-α that has been retained in cells. C8 B4 microglia were also encapsulated into 3D cultures using Matrigel and analyzed using an ELISA to distinguish any differences between the 2D and 3D cultures. The following time points were selected for this study: 60 minutes prior to the addition of LPS (-60 min.), simultaneously with LPS (t0), 30 minutes after LPS treatment (+ 30 min.), 60 minutes after LPS treatment (+ 60 min.), and 180 minutes after LPS treatment (+180 min.). A sample with no BFA treatment was used as the control. After allowing sufficient time for cytokine production and secretion, supernatants were collected and analyzed using a TNF-α ELISA. The cells were then fixed in paraformaldehyde (PFA) and stained for TNF-α. Representative images were taken and the average florescence

intensity per cell was measured using an automatic threshold method on ImageJ. Comparison of the ELISA and fluorescence results will allow us to select the optimal point to add BFA for spatial analysis studies in the future.

4.3 Results

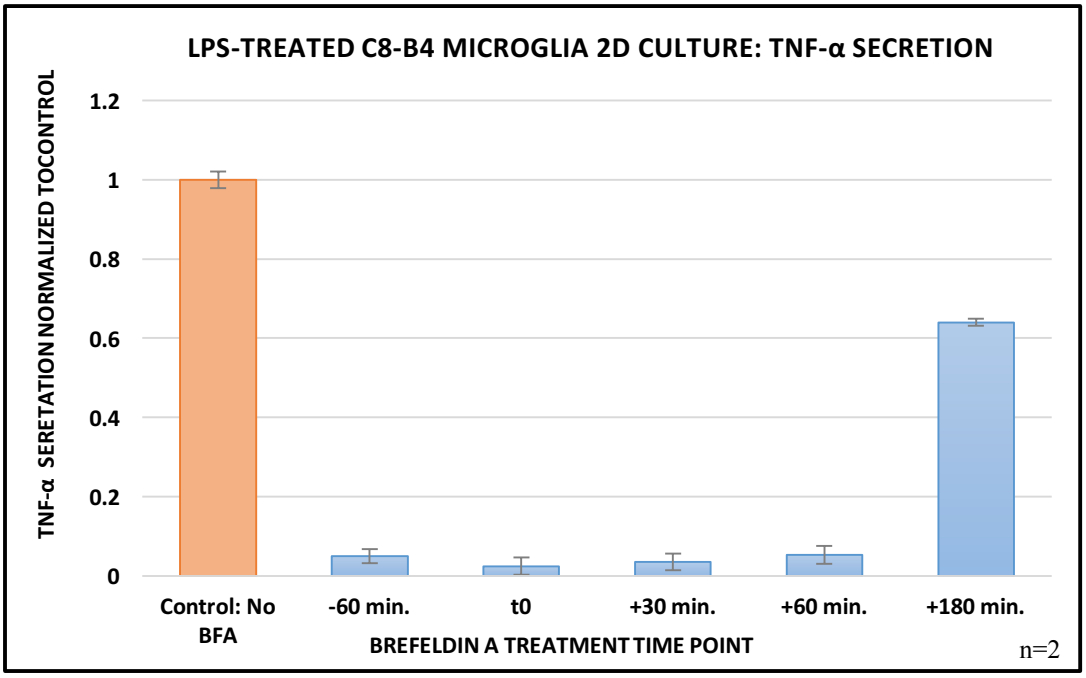

Figure 4.2: *BFA optimization experiment in LPS-treated C8-B4 microglia 2D culture. Values normalized to sample with no BFA treatment. Two replicates per time point.*

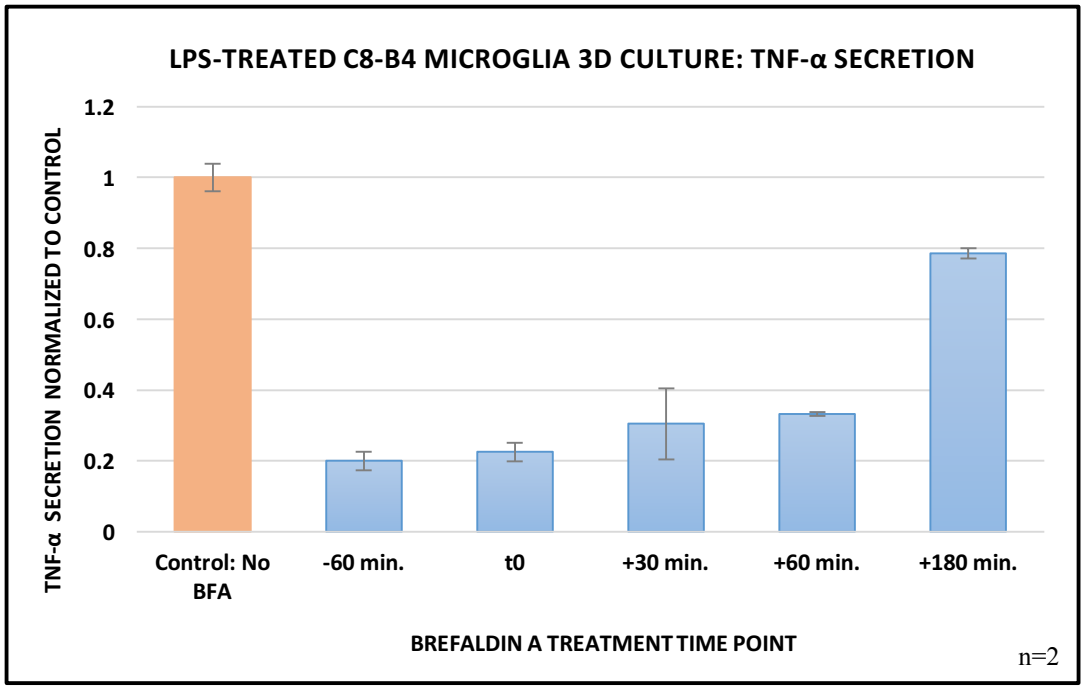

Figure 4.3: *BFA optimization experiment in LPS-treated C8 B4 microglia 3D culture. Values normalized to sample with no BFA treatment. Two replicates per time point.*

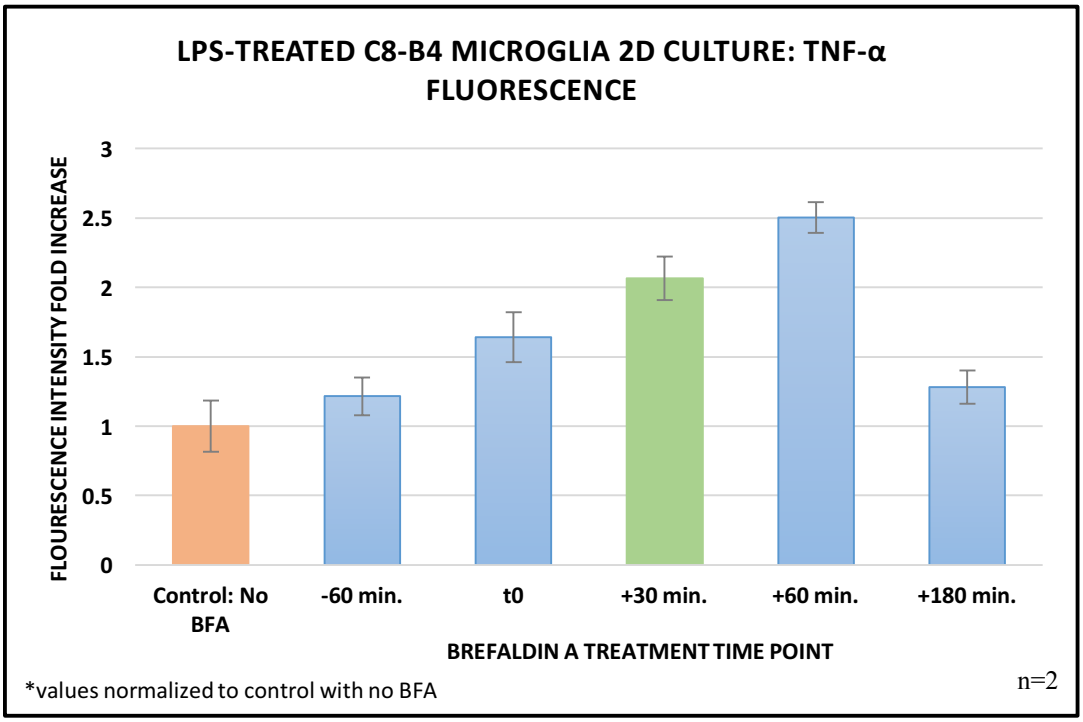

Figure 4.4: *TNF-α Fluorescence Intensity vs. BFA Treatment Time for LPS-Treated C8-B4 Microglia 2D Culture. Values normalized to sample with no BFA treatment. Two replicates per time point.*

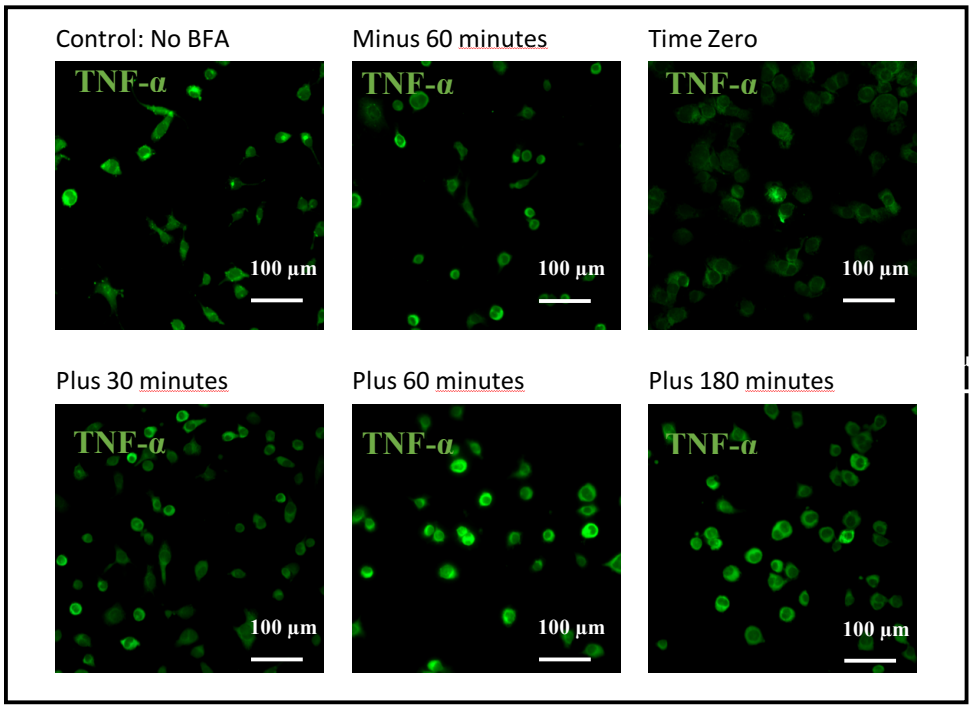

Figure 4.5: *Representative image of TNF-α-stained C8-B4 microglia at selected BFA treatment time points after LPS activation. Images taken at 200X at three representative areas per sample. N=2.*

4.4 Discussion

The ELISA results from the 2D culture **(Figure 4.2)** indicate there is a significant reduction in TNF-α secretion for time points -60 min., time zero, +30 min., and +60 min. compared to the control with no BFA treatment; TNF-α secretion is less than 10% compared to the untreated samples for these time points. This suggests that BFA was successful in retaining TNF-α within the cell, inhibiting secretion. We see that the TNF-α levels increase slowly as the time point of treatment is increased, perhaps because BFA has less time to inhibit secretion. At +180 min. however, there is a significant increase in TNF-α secretion. This suggests at this time point, majority of the TNF-α has been secreted out of the cells. **Figure 4.3** shows the same study with the 3D culture and a similar trend is seen, however the normalized values of TNF-α secretion are higher. This may be due to slower permeation of BFA through the hydrogel. A representative image for each time point after staining is shown in **Figure 4.5**. ImageJ analysis of the average florescence intensity per cell normalized to the control is shown in **Figure 4.4** and indicates that the signal is highest with BFA treatment 60 minutes after LPS activation; intensity values are approximately 2.5 times that of the control samples. Samples with treatment before this time point also have increased levels of fluorescence compared to the control with there being an increase in fluorescence intensity as the time of BFA treatment is delayed. However, at +180 min., values drop back closer to the control. This signifies that at this time point, TNF-α levels inside the cells are again lower. This matches the ELISA results discussed earlier where there was a sudden increase in TNF-α secretion. This suggests that majority of the in TNF-α produced by microglia are secreted prior to 180 minutes

after stimulation. Since this study did not include time points between +60 min. and +180 min., it is unknown whether after BFA treatment after 60 minutes and before 180 minutes of stimulation would increase or decrease TNF-α secretion. Additional time points can be investigated to provide better clarity. However, from this study alone, BFA treatment 30 minutes after stimulation is the safest choice and allows for a sufficient retention of TNF-α within the cell to produce a strong fluorescent signal. Therefore, using Brefeldin A appears to be a promising method for future spatial analysis studies to study local glial inflammation from fluid shear near the infusion site.

CHAPTER 5: CONCLUSIONS & FUTURE WORK

Through this study, we have accomplished to engineer innovative techniques to characterize the effects of fluid shear on tissue deformation and inflammation *in vitro*. We have implemented a computational technique called particle image velocimetry for flow detection and visualization that can detect low deformation magnitudes as a function of time and space using fluorescently-labeled agarose brain phantoms that mimic the mechanical properties of the brain. Additionally, although our attempt at bulk analysis of inflammation done in this study was not suitable in resolving inflammation at the local level, we have begun to develop a new biological approach using Brefeldin A to look at spatial analysis of inflammation that may better resolve local inflammation from fluid shear. The significance of this work is that it provides the building blocks to develop new and better tools to correlate tissue mechanics to inflammation for different kinds of brain implants and ultimately, it can provide a new approach for device characterization prior to *in vivo* studies. While our primary motive of developing these techniques is to determine feasibility and tolerance of specific flow rates for CED devices, the scope of this work is much broader as it can provide the insight necessary to translate CED devices into other applications in addition to oncology such as neuropsychology as new studies have now started developing microfluidic devices for treatment of seizure control [42].

However, the immediate future work for this project is to further develop the protocol for spatial analysis of inflammation. This involves developing a whole gel staining procedure or cryo-sectioning technique specific to Matrigel to analyze the 3D glial cultures at different cross-sections. Through our attempts, we have identified key issues such as preventing degradation of the gel through the fixation/cryo-sectioning process, preserving

gel structure when transferring the gel, optimizing incubation times for homogenous staining of the whole gel, and imaging within the well itself given the physical limitations of the microscope to be challenges that need to be overcome. Once these issues have been addressed and the technique has been developed, infusion studies can be performed and analyzed for spatial resolution of inflammation and these results can be overlaid with the tissue deformation studies to understand if low magnitude tissue deformation from fluid shear can lead to inflammation of glial cells and pose biological limitations that need to be considered. We can also explore adding neuron and and astrocytes into the cell model to obtain an even more physiologically representative microenvironment. Additionally, as we continue to develop new catheter designs for CED, it may be interesting to see if these new designs can combat backflow and in result increase the region of drug distribution. This can potentially lead to larger spatial deformation of brain tissue compared to what was seen in this study. If this is the case, it may be interesting to revisit the bulk analysis technique and see if it can detect inflammation response since a larger area of tissue deformation may be involved.

APPENDIX: DETAILED MATERIALS & METHODS

Chapter 2: Particle Image Velocimetry for Quantitative and Spatial Analysis of Brain Tissue Mechanics from Fluid Shear

A. Particle Image Velocimetry Analysis

i. Experiment Setup

24 well-plates (Corning) were drilled using a 61Y size drill bit to have a hole on the side of the well. A 3D printed clamp was used to ensure correct placement. Miniature polyimide tubing (Cole-Parmer, 24 AWG, .0201") was glued into the hole using UV epoxy (Loctite) and cured using ultraviolet light. This facilitates the insertion of a 27-gauge butterfly catheter needle (Exel) for infusion. 0.2% agarose solutions were made in 1X phosphate buffered saline (PBS, Gibco) and fluorescent red latex beads (Sigma-Aldrich, 2μm) were added to the solution at dilution of 1:25000. Solution was microwaved at increments of 10 seconds to ensure complete dissolution of the agarose. 1ml of solution was poured into the modified well-plates in order to achieve a gel height of at least 3mm. A programmable syringe pump (Harvard Apparatus PHD 2000) was used to infuse 10 μL of water at flow rates of 1 μL/min, 10 μL/min, 100 μL/min, and 500 μL/min.

ii. Data Acquisition & Analysis

Using the Zeiss Apotome.2 microscope and the 1.0X objective lens, time series images were taken for the flow rates

before, during, and after infusion. Infusion was started five seconds after starting the image capture. Three replicates were done per flow rate.

An open source application on MATLAB, PIVlab (Version 1.43 by W. Thielicke and E.J. Stamhuis, 2014) was used for analysis. Images were converted into binary form using ImageJ. The image stack was then uploaded into PIVlab. Images were calibrated using the scale bar for distance and image acquisition rate for time. Default integration settings were used for analysis which generates velocity vectors for each frame. Vector calibration is performed manually on each frame to remove noise and ensure that the vectors are within the correct magnitude range and the plot appearance was modified as appropriate. Values for velocity magnitudes, shear rates, and strain rates were derived along lines transversal and radial to needle geometry for each frame. Plots of velocity magnitude as a function of distance from the needle tip were generated using the frame that contained the maximum velocity magnitude. To calculate deformation over time, tangential velocity was derived for each frame at several points relative to the needle tip. Ensuring that similar trends are seen at these locations, plots were generated selecting a point 100 μm away horizontal from the needle tip and converted to displacement using the elapsed time obtained from the image acquisition rate. Displacement values prior the time point are

added together to obtain the net deformation at each frame. Additionally, using the velocity magnitude, heat maps were derived to provide spatial information using appropriate threshold criteria for each trial.

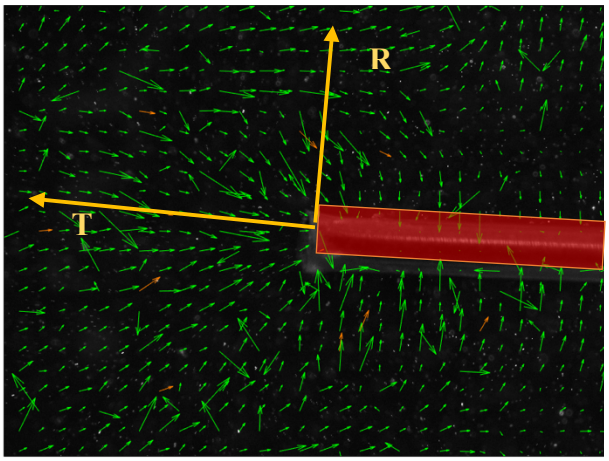

Figure A. *Illustration of how vectors were calculated along lines transversal and radial to needle geometry.*

C. Backflow Analysis (Courtesy of Dr. Sy's 2017 Senior Design Team)

0.6% agarose phantoms were made as described previously in modified 6 well plates that facilitate the insertion of a needle. Bromophenol blue dye (0.1 w/v%) was used to track the path of the fluid. An optical microscope was used to capture before and after images of infusion. Using ImageJ, the before and after images were overlaid and subtracted from each other. The resulting image was converted into a binary image and the mean gray value intensity profile was plotted as a function of distance. The location of the needle tip was identified and the area under the curve before and after the needle tip was integrated which correlates to

the volume of dye present in front and behind the needle tip. The percent backflow was calculated to be the volume of dye before the needle tip over the total dye volume.

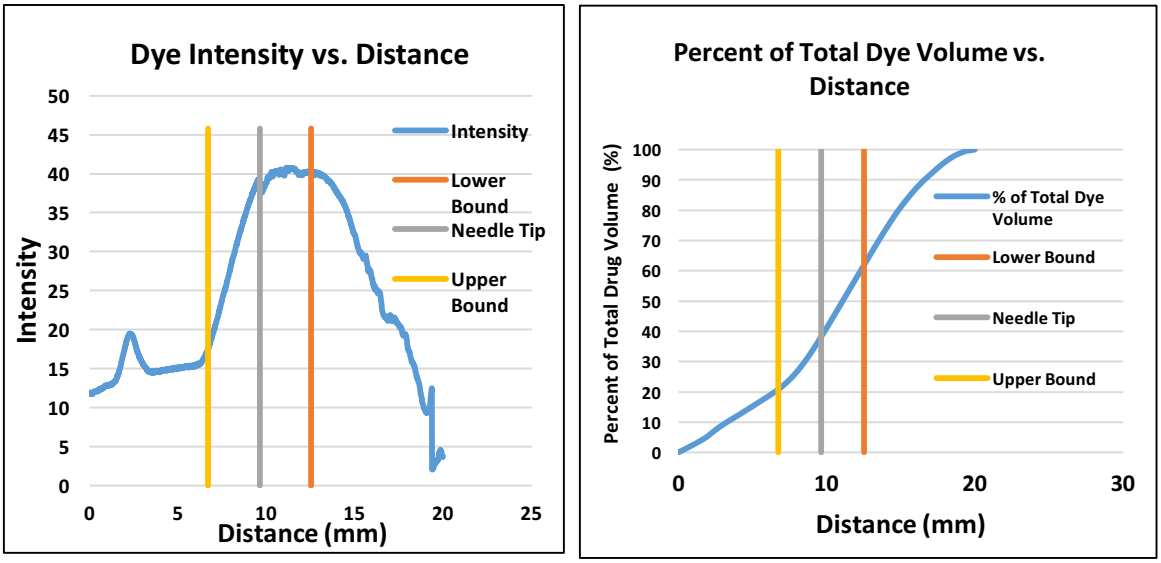

Figure B. *Sample plots of dye intensity relative to the distance from the needle tip (left) and percent of total dye volume relative to distance from the needle tip (right) generated to calculate percent backflow for selected flow rates.*

Chapter 3: Bulk Analysis of TNF-α for Quantification of Brain Inflammation from Fluid Shear

A. Cell Culture

C8 B4 mouse microglial cells were cultured in media containing DMEM (Gibco), 10% FBS (Fetal Bovine Serum, Gibco), and 1% Penicillin Streptomycin Glutamine (Gibco). Media was changed 3 times per week. Cells were expanded in T-150 flasks (Corning).

B. Encapsulation of Cells into 3D Matrigel Cultures

Cells were detached from the flasks by adding trypsin-EDTA (Gibco) for 5-10 minutes, counted using a hemocytometer, and seeded at a concentration of 3.75 million cells per mL. Aliquots of Matrigel were thawed in ice prior to the start of encapsulation. All tips were placed in the freezer at -20˚C in order to prevent gelification during the encapsulation process and cell-gel mixtures were made on ice. Matrigel was diluted to a concentration of 4.2 mg/ml based on previous preliminary rheology studies. Cell-Matrigel mixtures were plated onto a 24-well plate at a volume of 0.6 ml per well. The final gel dimensions were 15.6 mm in diameter and 3 mm thick. Gels were placed in the incubator at 37˚C to set for 20 minutes. Afterwards, 500uL of media was added to the top and changed every 2-3 days until the end of the experiment.

C. Live/Dead Assay: Imaging & Analysis

1.5µL of Calcein (1mg/ 200 µL) which stains green (excitation at 488 nm) for live cells and 1.5µL Ethidium Homodimer (1mg/ 233µL) which stains red (excitation at 594 nm) for dead cells were mixed into 500 µL of media and added to the gels. Gels were incubated in 37˚C for 20 minutes. Gels were washed with 1X sterile PBS and media was removed. Images were taken in the dark using the Zeiss Apotome.2 and the 1.0X lens. Images were taken at 3 different areas with magnifications of 20X, 40X, and 80X. Z-stack images were also taken throughout the depth of the gel at each area in increments of 10-30 µm to ensure that there was no significance change in the viability throughout the depth of the gel. Using the 40X images, the number of live and dead cells were counted manually using ImageJ

and the average of the three areas was used to calculate percent viability (number of live cells/ number of total cells X100). Representative images were taken at 3 areas for each sample. Images were taken at 24 hours, 48 hours, and 72 hours. Three samples were analyzed per time point.

D. *In Vitro* Infusion Experiment Setup

A microenvironment to simulate the immune response is created by modifying well plates to have a hole drilled on the side as done for the tissue mechanics studies in Chapter 2. This setup was sterilized using ethylene oxide (courtesy of The New Jersey Center of Biomaterials, Rutgers University). A programmable syringe (Harvard Apparatus PHD 2000) is used to infuse media with the selected flow rates, infusion duration, and volume as described in **Table 3.1**. Experiments were conducted in the cell culture incubator (37 ˚C, 5% CO_2) and left for 6 hours. LPS (Invitrogen) is diluted 1:10 in sterile PBS and then diluted in media to 10 μg/mL. LPS-treated samples will be used as a positive control whereas cells with no infusion will be used as the negative control. Each sample was done in triplicates. For samples with varying volumes of media infused, media was removed with and replaced with 300 μL of fresh media immediately after infusion to keep the dilution constant.

D. *Bulk Quantification of TNF-a Secretion*

Supernatants were collected for each sample 6 hours after LPS activation and stored at -80 ˚C. The supernatants were analyzed using a mouse TNF-α ELISA kit (Biolegend) following the manufacturer's instructions.

Chapter 4: Brefeldin A for Spatial Analysis of Brain Inflammation from Fluid Shear

A. Experimental Setup

Coverslips were placed in a 24 well plate and C8 B4 cells were seeded at a density of 3.75 X 10^6/mL for the 2D culture. 3D Matrigel cultures were also made using the protocol from Chapter 3. LPS (10μg/ml) was used to activate the the cells. A sample with no BFA added was used as the control. Samples were done in duplicates. BFA (10 μg/ml) was added at various time points: 60 minutes prior to the addition of LPS, simultaneously with LPS (time zero), 30 minutes after LPS, 60 minutes after LPS, and 180 minutes after LPS. Total volume of media was kept constant at 300 μL. The samples were incubated for 6 hours in order to allow for the production of cytokines. Supernatants were collected and analyzed using a TNF-α ELISA kit (Biolegend) following the manufacturer's instructions. Results were normalized to the control.

B. Immunofluorescence

The cells were fixed using 4% paraformaldehyde (PFA) for 10 minutes. To stain the cells for TNF-α, cells were first permeabilized with .1% Triton/PBS

for 10 minutes and washing 3X with PBS. The cells are then blocked with 1%BSA/PBS for one hour in 4˚C. Samples are again washed 3X with PBS for 5 minutes. Cells were incubated with the primary antibody, rabbit anti-TNF-alpha (Abcam, 1 μg/ml) in 1% BSA in PBST overnight at 4˚C. After 3X washing with PBS, cells were incubated with the secondary antibody, Alexa Fluor 488 donkey anti-rabbit (Abcam, 2μg/ml) for 1 hour in the dark. Cells were again washed and mounted with DAPI (300 nM). Coverslips were mounted onto microscope slides and fluorescence was analyzed using the Zeiss Apotome.2 with the 2.3X objective lens. Controls with only secondary antibody staining were used to set imaging parameters. Three different areas were imaged at magnifications of 50X, 100X, and 200X. Using the 100X images, cells were isolated using a color intensity threshold on ImageJ. The average mean gray scale intensity per cell was calculated for each condition. Results were normalized to the control.

REFERENCES

1. Chen, Y. and L. Liu, *Modern methods for delivery of drugs across the blood-brain barrier.* Adv Drug Deliv Rev, 2012. **64**(7): p. 640-65.

2. Cima, M.J., et al., *Single compartment drug delivery.* Journal of Controlled Release, 2014. **190**: p. 157-71.

3. Vogelbaum, M.A. and M.K. Aghi, *Convection-enhanced delivery for the treatment of glioblastoma.* Neuro Oncol, 2015. **17 Suppl 2**: p. ii3-ii8.

4. Debinski, W. and S.B. Tatter, *Convection-enhanced delivery for the treatment of brain tumors.* Expert Rev Neurother, 2009. **9**(10): p. 1519-27.

5. Karumbaiah, L., et al., *The upregulation of specific interleukin (IL) receptor antagonists and paradoxical enhancement of neuronal apoptosis due to electrode induced strain and brain micromotion.* Biomaterials, 2012. **33**(26): p. 5983-96.

6. Casanova, F., P.R. Carney, and M. Sarntinoranont, *Effect of needle insertion speed on tissue injury, stress, and backflow distribution for convection-enhanced delivery in the rat brain.* PLoS One, 2014. **9**(4): p. e94919.

7. Linninger, A.A., et al., *Prediction of convection-enhanced drug delivery to the human brain.* J Theor Biol, 2008. **250**(1): p. 125-38.

8. Kohn, J.C., et al., *Cooperative effects of matrix stiffness and fluid shear stress on endothelial cell behavior.* Biophys J, 2015. **108**(3): p. 471-8.

9. Moshayedi, P., et al., *The relationship between glial cell mechanosensitivity and foreign body reactions in the central nervous system.* Biomaterials, 2014. **35**(13): p. 3919-25.

10. Mehta, A.M., A.M. Sonabend, and J.N. Bruce, *Convection-Enhanced Delivery.* Neurotherapeutics, 2017. **14**(2): p. 358-371

11. Morrison, P.F., et al., *Focal delivery during direct infusion to brain: role of flow rate, catheter diameter, and tissue mechanics.* Am J Physiol, 1999. **277**(4 Pt 2): p. R1218-29.

12. Lueshen, E., et al., *Backflow-free catheters for efficient and safe convection-enhanced delivery of therapeutics.* Med Eng Phys, 2017. **45**: p. 15-24.

13. Kyriacou, S.K., et al., *Brain mechanics for neurosurgery: modeling issues.* Biomech Model Mechanobiol, 2002. **1**(2): p. 151-64.

14. Pomfret, R., G. Miranpuri, and K. Sillay, *The substitute brain and the potential of the gel model.* Ann Neurosci, 2013. **20**(3): p. 118-22.

15. Lee, H., et al., *Biomechanical analysis of silicon microelectrode-induced strain in the brain.* J Neural Eng, 2005. **2**(4): p. 81-9.

16. Lonser, R.R., et al., *Convection-enhanced delivery to the central nervous system.* J Neurosurg, 2015. **122**(3): p. 697-706.

17. Subbaroyan, J., D.C. Martin, and D.R. Kipke, *A finite-element model of the mechanical effects of implantable microelectrodes in the cerebral cortex.* J Neural Eng, 2005. **2**(4): p. 103-13. 1.

18. Spencer, K.C., et al., *A three dimensional in vitro glial scar model to investigate the local strain effects from micromotion around neural implants.* Lab Chip, 2017. **17**(5): p. 795-804.

19. Rothhammer, V. and F.J. Quintana, *Role of astrocytes and microglia in central nervous system inflammation. Introduction.* Semin Immunopathol, 2015. **37**(6): p. 575-6.

20. Polikov, V.S., et al., *In vitro model of glial scarring around neuroelectrodes chronically implanted in the CNS.* Biomaterials, 2006. **27**(31): p. 5368-76.

21. Puschmann, T.B., et al., *Bioactive 3D cell culture system minimizes cellular stress and maintains the in vivo-like morphological complexity of astroglial cells.* Glia, 2013. **61**(3): p. 432-40.

22. Placone, A.L., et al., *Human astrocytes develop physiological morphology and remain quiescent in a novel 3D matrix.* Biomaterials, 2015. **42**: p. 134-43.

23. Lieff, J. *Are Microglia the Most Intelligent Brain Cells*. 2013; Available from: http://jonlieffmd.com/blog/are-microglia-the-most-intelligent-brain-cells.

24. *Hydrogels for 3D cell culture*. Available from: https://www.sigmaaldrich.com/technical-documents/articles/biology/3d-hydrogels.html.

25. Feng, Y., et al., *Measurements of mechanical anisotropy in brain tissue and implications for transversely isotropic material models of white matter.* J Mech Behav Biomed Mater, 2013. **23**: p. 117-32.

26. Schomberg, D., et al., *Ramped-rate vs continuous-rate infusions: An in vitro comparison of convection enhanced delivery protocols.* Ann Neurosci, 2013. **20**(2): p. 59-64.

27. Krauze, M.T., et al., *Reflux-free cannula for convection-enhanced high-speed delivery of therapeutic agents.* J Neurosurg, 2005. **103**(5): p. 923-9.

28. Jahanmiri, M., *Particle Image Velocimetry: Fundementals and its Applications*. 2011, Chalmers University of Technology.

29. Thielicke, W. and Stamhuis, E.J. (2014): PIVlab – Towards User-friendly, Affordable and Accurate Digital Particle Image Velocimetry in MATLAB. *Journal of Open Research Software* 2(1):e30

30. LaPlaca, M.C., et al., *High rate shear strain of three-dimensional neural cell cultures: a new in vitro traumatic brain injury model.* J Biomech, 2005. **38**(5): p. 1093-105.

31. Alliot, F., et al., *A spontaneously immortalized mouse microglial cell line expressing CD4.* Brain Res Dev Brain Res, 1996. **95**(1): p. 140-3.

32. Xu, X., J.A. Kim, and Z. Zuo, *Isoflurane preconditioning reduces mouse microglial activation and injury induced by lipopolysaccharide and interferon-gamma.* Neuroscience, 2008. **154**(3): p. 1002-8.

33. Nguyen, N.T., et al., *Proenergetic effects of resveratrol in the murine neuronal cell line Neuro2a.* Mol Nutr Food Res, 2013. **57**(11): p. 1901-7.

34. Benton, G., et al., *Matrigel: from discovery and ECM mimicry to assays and models for cancer research.* Adv Drug Deliv Rev, 2014. **79-80**: p. 3-18.

35. Haw, R.T., et al., *A three-dimensional collagen construct to model lipopolysaccharide-induced activation of BV2 microglia.* J Neuroinflammation, 2014. **11**: p. 134.

36. East, E., J.P. Golding, and J.B. Phillips, *A versatile 3D culture model facilitates monitoring of astrocytes undergoing reactive gliosis.* J Tissue Eng Regen Med, 2009. **3**(8): p. 634-46.

37. Gautam, J., X. Zhang, and Y. Yao, *The role of pericytic laminin in blood brain barrier integrity maintenance.* Sci Rep, 2016. **6**: p. 36450.

38. Shih, R.H., C.Y. Wang, and C.M. Yang, *NF-kappaB Signaling Pathways in Neurological Inflammation: A Mini Review.* Front Mol Neurosci, 2015. **8**: p. 77.

39. Jose Enrique Yuste, E.T., Carmen Maria Campuzano, Francisco Ros-Bernal, *Implications of glial nitric oxide in neurodegenerative diseases.* Friontiers in Cellular Neuroscience, 2015.

40. Klausner, R.D., J.G. Donaldson, and J. Lippincott-Schwartz, *Brefeldin A: insights into the control of membrane traffic and organelle structure.* J Cell Biol, 1992. **116**(5): p. 1071-80.

41. Jocelyn K.C. Rose, S.-J.L., *Straying off the Highway: Trafficking of Secreted Plant Proteins and Complexitiy in the Plant Cell Wall Proteome.* American Society of Plant Biologists, 2010. **153**(2): p. 433-436.

42. Proctor, C.M., et al., *Electrophoretic drug delivery for seizure control.* Sci Adv, 2018. **4**(8): p. eaau1291.